CREEP BEHAVIOR OF FIBER REINFORCED SELF CONSOLIDATING CONCRETE REINFORCED WITH HYBRID FIBERS

By

JONATHAN F RODRIGUEZ

A thesis submitted to the

School of Graduate Studies

Rutgers, the State University of New Jersey

In Partial Fulfillment of the requirements

For the degree of

Master of Science

Graduate Program in Civil & Environmental Engineering

Written under the direction of

Dr. Hani Nassif

And approved by

_____

_____

_____

New Brunswick, New Jersey

May 2019

ABSTRACT OF THE THESIS

Creep and shrinkage properties of fiber reinforced self-consolidating concrete (FR-SCC) are still unknown and limited in research. Thus, comprehensive evaluation is required to determine these behaviors of FR-SCC and mechanical properties must be verified to determine effectiveness of this type of concrete in structural application.

The objective of the research is evaluation of the influence of micro/macro polypropylene and steel fibers on creep and shrinkage of self-consolidating concrete. (8) mixes are performed with recommended dosages of fiber content; and two mixes will be hybrid combination of the fibers with appropriate fiber dosages. Concrete specimens were also evaluated for fresh concrete property testing such as slump, j-ring, visual stability index, T20 and air content (pressure method) and for mechanical properties such as compressive strength, tensile strength, elastic modulus, free shrinkage, flexure, and rapid chloride permeability testing.

Experimental data for creep and shrinkage were also compared to the following prediction models: ACI209, B3, CEB MC90-99. and GL2000 to determine which model most accurately predicts the behavior of these FR-SCC mixes. Results show that a combination of micro and macro polypropylene fibers cause the most reduction in shrinkage but also cause the most increase in creep strain compared to non-fiber-reinforced self-consolidating concrete. Furthermore, polypropylene fibers of 1.5" length cause the highest increase in specific creep while steel crimped fibers of 1.5" length cause the lowest increase in specific creep. Finally, Bazant-Baweja B3 Model is the most accurate model in predicting creep behavior for the FR-SCC mixes while CEB90-99 is the most accurate for predicting shrinkage behavior for FR-SCC

mixes. A correction equation is implemented for the Bazant B3 creep model to increase accuracy of prediction to experimental data.

ACKNOWLEDGEMENTS

The following thesis was completed under the guidance of Professor Hani H. Nassif of the department of Civil and Environmental Engineering. I would like to thank Dr. Nassif for providing me the opportunity to work with him as an undergraduate and graduate research assistant and the constant encouragement and support during the progression of writing this thesis.

I would also like to thank Dr. Hani Nassif, Dr. Husam Najm, and Dr. Adi Abu-Obeidah for being members of my committee.

I would also like to thank the undergraduate research assistants for the significant amount of help provided throughout the experimental stage of the research including mixing, testing and maintenance work. I would especially like to show my gratitude for Dr. Adi Abu-Obeidah who, since my very first day of research, has served as a great mentor and supervisor with his experience and knowledge that I will never forget.

Finally, I thank my family and friends for their care and love throughout my time here at Rutgers University.

TABLE OF CONTENTS

LIST OF TABLES

LIST OF FIGURES

CHAPTER I

1. INTRODUCTION

1.1 **Problem Statement**

Self-consolidating concrete (SCC) is defined as fresh concrete with exceptional flow ability without sacrificing stability of the mix (Goodier 2003). It is characterized mainly through the following traits: flowing ability, passing ability, and resistance to segregation. Self-consolidating concrete mixes can fill all areas of formwork and can pass through very congested reinforcement without blockage. Additionally, it can retain its components in suspension for ensuring homogeneity. Utilizing self-consolidating concrete eliminates the need for vibration and, consequently, reduces labor costs since placement of the concrete becomes much faster and at a much more convenient rate. As of now, it is proven to be highly profitable and productive mainly due to the shortened construction period and reduced noise of vibration, especially in local areas (Goodier 2003). On the other hand, because of the high dosage of high range water reducer, self-compacting concrete mixes can “bleed” during the mixing phase in which water and aggregates begin to segregate from the mix itself, causing severe loss in strength. Furthermore, self-consolidating concrete has a high risk of plastic shrinkage cracking due to the high amount of shrinkage that occurs.

All forms of concrete subjected to a sustained load continuously deform over time; this is the basic definition of the creep phenomenon, discovered by Hatt in 1907 (Bazant 1975). Moreover, concrete also exhibits shrinkage, the volumetric deformation due to water content reduction and the chemical processes concrete undergoes as it cures. Creep and shrinkage distinguish based on

the condition of the concrete, yet both play an important role in influencing concrete as it cures and maintains form over time, especially for years and years on end (Bazant 1975). Both creep and shrinkage are very prevalent issues with SCC mixes due to the fact that they exhibit higher creep and shrinkage behavior than conventional concrete due to the high paste content and high w/c ratio (Aslani and Nejadi 2014).

Typically, fibers are added as a solution to shrinkage and creep problems while also increasing tensile strength. Common fiber materials can be steel, polypropylene, and glass; the type of fiber used can prioritize either more reduction in shrinkage or creep or both. The primary disadvantage of including fiber content to a mix is the severe loss of slump and workability of the mix leading to blockage and clumping during the casting process (Khayat 1999).

Research regarding self-consolidating concrete is still recent, especially with the involvement of fibers within the mix. Furthermore, experimentation with the creep and shrinkage behavior of fiber reinforced self-consolidating concrete is still relatively new, and there have yet to be any theoretical models accurately predicting how the concrete creeps over time once fibers are added. Determining an effective creep prediction model can greatly encourage use of FR-SCC within the construction industry and may present greater practicality.

1.2 Research Objectives and Background

The objective of this research is the investigation of creep and shrinkage behavior of self-consolidating concrete varying in fiber type and quantity. This ranges from mixes including steel fibers, macro and/or micro polypropylene fibers, or a combination of both types. Furthermore, experimental analysis of the concrete creep behavior will be evaluated by the current ACI models available [ACI209R-92, Bazant Baweja-B3, GL2000, and CEB MC 90-99] and proper

adjustments to accurately predict fiber reinforced self-consolidating concrete creep behavior is recommended. All materials are gathered locally within New Jersey and in a cost-effective manner while ensuring high quality standard concrete that is satisfactory for practical use in the construction industry. A total of 8 mixes are investigated, each with a different fiber type, length, dosage or combination.

1.3 Thesis Organization

This thesis has six chapters as followed:

Chapter I:

An introduction and concise background to the scope of the research and thesis objective.

Chapter II:

Literature background on self-consolidating concrete, the steel and polypropylene fibers, types of strains involved in concrete, an explanation of the creep mechanism, and a background of the following ACI Creep Models: ACI209R-92, Bazant Baweja-B3, GL2000, and CEB MC 90-99

Chapter III:

Overview of the experimental stage of the research including information on the mixes performed, testing performed, and the appropriate setup for acquiring creep and shrinkage data over a period of one year.

Chapter IV:

Review of the results, including immediate and mechanical properties, analysis of the creep and shrinkage behavior for each mix and a discussion on the influence from each fiber type.

Chapter V:

Comparison between experimental data and creep and shrinkage models simulating theoretical creep and shrinkage behaviors is made. Furthermore, the most accurate prediction model is stated as well as what appropriate correction is needed on the models.

Chapter VI:

Conclusion of the thesis providing possible future workings to continue this research and relevant recommendations.

CHAPTER II

2. LITERATURE REVIEW

2.1 Introduction

A literature review on self-consolidating concrete, fiber types, creep and shrinkage behavior, and ACI creep prediction models is provided within this chapter. The benefits and worth of self-consolidating concrete and fibers are discussed as well as their disadvantages. Furthermore, the phenomenon of creep and shrinkage in concrete structures is also explained as well as factors that influence these behaviors. Finally, four ACI creep and shrinkage prediction models are reviewed in detail.

2.2 Self-Consolidating Concrete (SCC)

In 1988, self-consolidating concrete was created to provide more durable concrete structures with an improved construction process. This was accomplished by removing the need to compact and use vibration techniques performed in traditional concrete construction processes. Self-consolidating concrete was meant to accommodate the lack of skilled site workers in the industry during this time and allowed faster construction and eliminated vibration noise issues (Goodier 2003). Therefore, the introduction of this new type of concrete offered economic, social, and environmental advantages. Around the late 1990s, Sweden became the first country in Europe to encourage the development of self-consolidating concrete since several studies presented its use to reduce bridge construction costs by about 15% and reduce energy consumption and greenhouse gas emissions by 30% (Goodier 2003). Consequently, self-consolidating concrete was introduced to several other European countries and by around the early 2000 it reached academic institutions for further development (Goodier 2003). As of now,

self-consolidating concrete development has reached even Canada and North America, and it is currently spreading to South America. Researchers have stated the main barrier of self-consolidating concrete usage is that there is a lack of experience in the process and a lack of published guidance, codes and specifications (Goodier 2003).

A typical concrete mix includes a combination of cementitious materials, water, aggregates and various admixtures functioning to add benefits to a concrete mix or greatly manipulate its properties ("Scientific Principles").

Cement is a mixture of compounds formed by burning limestone and clay. It is mixed with water to form the binding paste of concrete during its formation as the water stimulates hardening of the cement through hydration in which the major compounds form chemical bonds with water molecules to become hydration products ("Scientific Principles"). The breaking and forming of chemical bonds during hydration generates heat, particularly during the first day of the mix being formed. The hydration process is slow and continuous as the concrete hardens and increases in strength; and water in the form of moisture must always be present until the process is complete so that the concrete acquires its distinctive compressive strength. The water to cement ratio is the most critical factor for ensuring a high-quality concrete mix since this determines the overall strength of the concrete as well as its workability ("Scientific Principles"). The workability is defined as the concrete's ability to consolidate and form into different shapes ("Scientific Principles"). The less water used, the stronger the concrete, and the more water, the more workable the concrete is. An effective concrete mix will be both strong and workable to satisfy industry and structural standards ("Scientific Principles").

In self-consolidating concrete mixes, the water to cementitious material ratio becomes even more critical in providing the balance between the required strength and flow ability. W/C

ratios are typically higher for such mixes to give its distinct fresh properties, but the mix is also extremely delicate as adding more quantity of water afterwards can quickly result in the segregation of the concrete in which the coarse aggregates separate from the uniform mix during curing. Hence, using proper dosage of high-range water reducing admixtures is very vital to have better flowing ability without risking segregation and uniformity.

The aggregates are the solid particles held together by the cement paste and act as the filler of the concrete. Due to its high cost, cement is the ingredient that must be minimized in concrete, and in its place is the aggregates that make up more than half the volume. Selection of aggregates is based on the required characteristics of the concrete mix and as a result, aggregates are separated into various sizes for better organization of selection. Generally, aggregates are divided into coarse and fine types due to the vast difference in influence each of them has on a mix ("Scientific Principles").

Regarding self-consolidating concrete, use of coarse aggregate material plays a vital role in its fresh and hardened properties. SCC is very sensitive to coarse aggregate characteristics such as shape, texture, max size and grading since the mix must prioritize workability. Increasing the size of coarse aggregates can ruin the flow ability of SCC with blockage and segregation issues (Khalell, et al, 2011). Because of this downfall, fine aggregates are used in higher proportions compared to conventional concrete mixes to insure granular continuity.

In addition to cement, a concrete mix may have other cementitious materials including, fly ash and slag that can combine with cement to produce other properties to the concrete. Slag cement is hydraulic cement created from granulated blast furnace slag (GGBFS) grounded to a certain fineness with the purpose of replacing a portion of Portland cement (Boukendakji, Kenai, Kadri, Rouis, 2009). Ground granulated blast-furnace slag is glassy and contains silicates and

alum inosilicates developed in molten conditions. The granulated slag must be very finely grounded to be of use in concrete and provide the proper benefits. The component tends to respond well with air entrainment admixtures up to a certain extent unless it is excessively fine ("Ground Granulated Blast-Furnace Slag: Its Chemistry and Use with Chemical Admixtures"). As GGBFS is added to the mixture, it reacts with water to produce chemical compounds increasing the durability of the concrete; but the gain is only noted after the 28-day mark. GGBFS is classified into three strength grades, grade 80, 100, and 120 in accordance to ASTM C989 ("Ground Granulated Blast Furnace Slag"). Among the measurable improvements for adding slag are better workability, higher compressive and flexural strengths, lower permeability, and better plastic properties **(**Boukendakji, Kenai, Kadri, Rouis, 2009**)**.

Ground granulated blast-furnace slag in SCC mixes greatly increases the concrete workability and can consequently reduce the necessity of water reducing admixture dosages while maintaining the proper water/cement ratio. Furthermore, GGBFS offers the benefit of enhancing the grain size distribution and cohesiveness to the mix, which facilitates the overall needed stability. Unfortunately, the inclusion of slag reduces compressive strength compared to self-consolidating concrete purely mixed with cement **(**Boukendakji, Kenai, Kadri, Rouis, 2009**)**. On the other hand, a higher percentage of slag used, regardless of grade, yields lower total shrinkage, drying plus autogenous, in concrete after about 1 year ("Ground Granulated Blast Furnace Slag").

High range water reducing admixtures, or superplasticizers, are soluble macromolecules much larger than water molecules that use the process of adsorption to perform their function ("Plastol 5000: High Range Water Reducing Admixture"). Water reducing agents influence the water to cement ratio by reducing the amount of water added so that the cement paste gains a

higher density. Consequently, a higher density yields more strength, durability and shrinkage of concrete which is why HRWR agents are so vital in the industry today. It is a proper alternative to adding water without lowering the workability of concrete and modifying its properties for better suitability ("Use of Water Reducers, Retarders, and Superplasticizers). Superplasticizer is the key ingredient for providing self-consolidating concrete with its flow ability while making it viable for structural application.

Concrete with air entrainment admixture contains a controlled amount of air in the form of microscopic bubbles ranging in size from a thousandth of an inch to a few hundredths. The admixture acts as a lubricant with the air bubbles behaving like flexible ball bearings assisting sand and aggregate particles to slide past one another. AEA admixtures give concrete extra workability and permits use of less water and sand in a mix which is encouraged for SCC mixes because it can help prevent excessive bleeding, which is when water appears on the surface of the mix, weakens the wearing surface of the concrete, and causes segregation of the aggregates ("How to Use Air-Entrained Concrete"). Additionally, air entrained concrete forms a barrier to water movement on the surface that results in a more watertight concrete, giving the mix greater longevity and less maintenance. Arguably, the most important benefit to AEA is that it offers concrete more resistance to freeze-thaw damage and scaling due to de-icing salts and chemicals. Because concrete contains moisture that can expand in low temperatures, surface scaling may occur which can rupture concrete due to the large expansive forces. The small, entrained air bubbles serve as reservoirs to mitigate this pressure and help prevent scaling problems in real-world applications ("How to Use Air-Entrained Concrete").

The flow ability of SCC is measured with an adjusted version of the slump test following ASTM C 143 with a recommended spread of 18 to 32 inches. Two major properties specific for

SCC are flow ability and stability (NRMCA, 2004). Flow ability indicates the ease of flow without effort and is part of a mix's filling ability ("Definition of Terms Relating to Self-Consolidating Concrete"). High flow ability of SCC is achieved by using high-range-water-reducing (HRWR) admixtures without the need for additional water **.** Stability is defined as the ability to remain homogeneous throughout the entire process of mixing, casting and curing the concrete mix . It is acquired by increasing the quantity of fines usually achieved by increasing cementitious content or by including mineral fines. Admixtures may also increase stability if they affect mixture viscosity; and they are much preferred over adding additional water since this may cause stability issues in addition to increased flow ability (NRMCA, 2004**).** SCC mixture proportions should meet adequate requirements of yield stress and plastic viscosity which provide its distinct filling ability and placement in congested sections (Khayat, 1999). SCC has reduced coarse aggregate content that is accommodated by increasing the volume of cementitious materials such as slag and fines such as sand. The incorporation of more powdered material improves packing density and reduces inter-particle friction which leads to the reduced viscosity of the mix while improving compaction and stability. Cohesiveness of the paste is also enhanced due to the reduced water/cement ratio in which water is replaced with high amounts of HRWR (Khayat, 1995).

2.3 Fibers

It has become a common practice for companies to reinforce concrete mixes with fiber materials to improve certain properties. During the early ages of concrete, volume changes can cause weak planes resulting in the formation of cracks (Wafa 1990). This is because concrete does not excel at tensile strength and has brittle characteristics. The growth of these cracks can be dangerous as they eventually result in the failure of the concrete specimen even with

compressive strengths much lower than what the specimen is supposed to handle. Therefore, cracks in concrete are an issue for its durability, serviceability, and appearance since their presence can be an instigation for disputes between owners, architects, and engineers due to its perception that it leads immediately to structural failure. The distribution of fibers in concrete mixes inhibits the formation of these cracks during the plastic stage and discourages large capillary developments stimulated by bleeding of the concrete (Wafa 1990).

Fiber is generally introduced to counter the issue of cracking that concrete undergoes because of how brittle the material can be during the plastic and hardened stages (Wafa 1990). They also provide a myriad of benefits ranging from improved tensile strength, lower permeability, enhanced resistance to shattering, impact, and abrasion and even minimizing the creep strain that occurs throughout the life of a concrete specimen. Fibers can also have small improvements to the compressive strength, flexure, toughness, and modulus of elasticity of a concrete specimen according to several experiments (Wafa 1990). However, in as much as fibers provide benefit to the mechanical properties of concrete, it is at the expense of the workability of the concrete mix. All types of fibers are shown to reduce the filing ability because the small material can block concrete from passing through densely reinforced areas during the casting stages. Increasing fiber dosage in mixes has been linked to also increasing HRWR dosages to accommodate for the reduced workability and ensure that standards are nevertheless met in immediate testing (Wafa 1990).

A wide variety of fibers exist for different applications in providing optimal usage. The two main types involved within this research study are synthetic and steel fibers. Under the synthetic fiber category, there are polypropylene, nylon, polythene, polyester, and glass fibers. On the other hand, steel fibers are manipulated by either having them straight, crimped, hooked, or

twisted to accommodate for the desired requirements (Wafa 1990). In this research study, only polypropylene synthetic and crimped steel fibers are involved.

The various lengths provided for the fibers are meant to optimize a balance between strength and fiber distribution and are commercially available from ranges of 0.5 to 2.5 inches. These types of synthetic fibers are very effective in holding the mix together and consequently reduce the rate of bleeding by slowing the settlement of coarse aggregate. Because of the reduced bleed rate, there is less plastic shrinkage cracking occurring within the concrete compared to mixes without fibers. During the casting process, polypropylene fibers affect the slump of concrete and can prolong the settling time; so, adjustments must always be made to allow the mix to satisfy fresh property standards. Once the concrete hardens, the fibers forms a three-dimensional reinforcement to distribute tensile stresses more uniformly and improve impact resistance, tensile and flexural strength, and lower the modulus of elasticity due to better ductility ("Concrete Reinforced with Polypropylene Fibers"). The polypropylene fibers can be classified into the categories of macro and micro-fibers. The macro fibers are more intended to replace reinforcement in certain non-structural applications. They minimize and even eliminate early and late age cracking and are usually at least 1.5 inches in length. Micro fibers are more intended for minimizing only early age cracking and, in addition to length, can also be categorized based on their aspect ratio ("Construction and Materials Tips").

Steel fibers provide very similar advantages and disadvantages to concrete like polypropylene fibers, which include increased tensile strength, greater ductility, but also a reduction in workability. However, steel fibers have been shown to provide more tensile strength to concrete compared to polypropylene fibers. Furthermore, some experimentations concluded that steel fibers are much more likely to increase compressive strength by 28 days, even by only

a small percentage. Unfortunately, the downfall of steel fibers is that ultimate deflection is significantly greater compared to any synthetic fiber type, and it is also not primarily intended for plastic shrinkage. In other words, the effects of steel fibers lean more towards increasing overall strength of the concrete rather than focusing on preventing shrinkage and crack formation as with polypropylene fibers (Hadi 2008).

2.4 Shrinkage and Creep

Because of the need to provide workability, concrete always uses a greater amount of mixing water than desired for its hydration process. As concrete hardens, this excessive water causes volume reduction in concrete, the phenomenon that is named concrete shrinkage. The major concern with shrinkage is cracking potential which may lead to serious structural issues throughout the age of the concrete ("Concrete Technology in Focus"). To explain in a general manner, cracking is always because of restraint; and the restraint can be applied externally or internally based on application. With the presence of cracks, aggressive chemicals may acquire access to the matrix of the concrete, thus reducing long term durability of a structure. Regarding practical application in the industry, shrinkage cracking is a detrimental effect, especially in dimensional stability and prestressing applications ("Concrete Technology in Focus").

Several types of shrinkage in concrete include plastic shrinkage, dry shrinkage, thermal contraction, autogenous shrinkage, and carbonation shrinkage. Shrinkage from thermal contraction occurs as the temperature of fresh concrete gradually cools to the ambient temperature while it hardens. Autogenous shrinkage is the result of the chemical reactions taking place during the cement hydration and can be very impactful with mixes that have very low water-cementitious materials ratio. Because of the insignificant magnitude of autogenous

shrinkage and thermal contraction, only plastic and dry shrinkage are primarily acknowledged in this research study.

Loss of water from fresh concrete can occur in many ways, mostly due to evaporation from the exposed surfaces. This generates negative capillary pressures causing the volume of the paste to contract, stimulating plastic shrinkage. The magnitude of this type of shrinkage is strengthened by several factors that similarly affect the rate of water evaporation which include humidity, ambient temperature and the temperature of the concrete. Crack formation is instigated due to plastic shrinkage should the rate of moisture loss exceed the rate at which bleeding water reaches the surface of the concrete, according to reports. Therefore, precautionary measures have been designed for controlling the crack formations primarily by reducing temperature within concrete and using fibers, especially those that are micro synthetic ("Concrete Technology in Focus").

Dry shrinkage is the loss of moisture after the concrete hardens and becomes a major consideration in structural design and construction. It is caused by the loss of absorbed water from the hydrated cement paste. As concrete is exposed to drying conditions in which there exists a difference in relative humidity between the environment and the concrete itself, the specimen initially loses free water. Large capillary pores within the concrete are not affected, but the finer water-filled capillary pores have the surface tension of the water pull the walls of the pores, developing internal negative pressure. The continued exposure of concrete to drying conditions leads to this ongoing process of surface tension as well as increased attraction forces between the hydration products. In addition to relative humidity, other factors such as the characteristics of the concrete mix ingredients, proportions, and other environmental influences may affect the rate of drying shrinkage ("Concrete Technology in Focus").

Creep is the time-dependent strain induced by a constantly applied stress over time. It is the non-elastic deformation increasing at a decreasing rate during a period of loading. In concrete specimens, creep is significant within the early ages and very minimal after years of applied loading. In fact, approximately 25% of total creep takes place during the first month of the sustained loading and 50% occurs for the first half year of sustained loading. Concrete that has its load removed does not return to its original state due to this phenomenon (Kumar and Kumar 2014).

Generally, creep is an undesirable trait since it leads to excessive deformation and deflection that requires costly repairs, especially in large prestressed concrete members. In fact, loss of prestress due to creep is widely known and accounts for many failures unless high tensile steel is utilized for reinforcement. For simple reinforced concrete columns, creep can result in the gradual transfer of load from concrete to the reinforcement. Hence, reinforcement may yield before the structure reaches its designed load of failure. Even when creep does not influence the ultimate strength of a structure, it can compromise the structural performance. In mass concrete, creep can be the sole cause of cracking if concrete that is restrained undergoes excessive cycles of temperature changes (Kumar and Kumar 2014).

Creep strain does not include any shrinkage, so experimentations regarding creep usually have focus on shrinkage as well usually by comparing loaded specimens with unloaded specimens under the same environmental conditions. In addition, the dual mechanism of creep is relaxation which is the time-dependent reduction of the applied stress. The following terms are commonly used in construction specifications regarding the phenomenon of creep: creep coefficient, compliance function, and specific creep. Creep coefficient expresses delayed deformation respective to elastic strain which is caused during the initial loading of the material.

Compliance function represents creep strain per unit of imposed stress to compare delayed strains taking place at different stress levels. Next, specific creep expresses only delayed strains due to the application of a unit stress. Regarding this study, specific creep is the primary term used for comparing results and determining the outcome of the research ("Drying Shrinkage and Creep in Concrete: Summary").

Traditionally, creep can be separated into two categories: basic creep deformation which is defined as deformation under constant load and constant humidity conditions and drying creep strain which is defined as the deformation in excess to basic creep as the concrete specimens are exposed to drying conditions while loaded ("Drying Shrinkage and Creep in Concrete: Summary"). Basic creep is strongly dependent on moisture content and shows two stages at macroscopic level. One stage is short term creep kinetics acting predominantly during the first days after load application and having a similar time scale to relaxation of creep. Some mechanisms have been proposed for explaining short term creep kinetics including osmotic pressure effect, theory of solidification, and migration of water within capillary porosity ("Drying Shrinkage and Creep in Concrete: Summary").

For osmotic pressure in cement paste to develop, there must exist a semipermeable gel layer between grain surfaces and capillary spaces as well as the presence of different ion concentrations in the capillary spaces. The gel occupies more space than the mineral from which it comes from and coating of the gel builds to several layers. Because of the physical properties of the gel and the conditions within and around the coating over cement grains, osmotic pressure develops; and if the grains hydrate, there exists a state of super-saturation (Ghosh 1973).

The solidification theory for aging creep considers aging because of volume change of load-bearing solidified material, which is hydrated cement in this case. To simplify, it can be assumed

that the volume of hydrated cement grows by the layer deposition of the material and that during solidification, a layer of the material must be stress-free (Bazant & Prasannan 1988). Material in the concrete must decompose into constituents of non-aging properties with aging relating to change in volume of a component. According to Bazant and Prasannan, the compliance function of the cement gel is the sum of viscoelastic strain and viscous flow characteristics and terms for the function are acquired in terms of rates. This is a means to explain how volume increase in the cement gel is very small, yet creep properties change significantly up to several years. As shown below, the compliance function can be combined with effects of aggregate to represent the theory of solidification: (Granger & Bazant 1995).

$$J_p(t,t_0) = \left(\frac{1}{E_P^0}\right) + \frac{1-b}{E_h} * \emptyset(t,t_0) + (\frac{b}{E_0^*})(\frac{E_h - R_h - \Delta_a E_a}{a(t)E_{ac} + E_h^n})$$

The second stage of the solidification theory is long term creep kinetics describing the pronounced aging period influenced only by the age of the material and not the age of loading. The most accepted mechanism for this stage is the micro-sliding between CSH particles and their respective sheets (“Drying Shrinkage and Creep in Concrete: Summary”).

2.5 Factors Influencing Creep

The rate of creep is influenced by several factors ranging from the material of the concrete mix to the proportions of the mix to environmental and loading conditions of the concrete over time.

Concrete made with low-heat cement tends to creep more than normal concrete due to the influence of the degree of hydration. Concrete has more of the tendency to creep less as the cement hydration increases. Using more slag and/or fly ash material within a mix reduces the

specific creep of the concrete, but the reduction provided by fly ash is slightly greater than the reduction provided by ground granulated blast furnace slag (Castel et al, 2016).

Creep decreases when using well-graded aggregates that have low void content and also when the coarse aggregate is of greater size with low absorption and high modulus of elasticity. Additionally, the mineral composition of the aggregate is valuable and can increase creep depending on the type; generally, creep increases the most with limestone, quartz, and granite compositions in the aggregate (Kumar and Kumar 2014).

Creep of concrete increases with increasing water-cement ratio and with mixtures that have greater volume of cement paste. As a result, “lean” concrete mixtures exhibit much more creep compared to “rich” concrete mixtures due to the water-cement ratio effect. Air entraining agents do not significantly affect the rate of creep but polycarboxylate superplasticizers, on the other hand, provide an impact (Qian et al 2016). Results show that superplasticizers refine capillary pores and reduce surface tension, thereby improving the hydration degree and decreasing porosity of macro pores (Qian et al, 2016). In other words, this admixture reduces the rate of creep. More specifically, the polycarboxylate superplasticizers, compared with naphthalene-based plasticizers, cause greater reduction of drying creep and a smaller reduction of basic creep due to the moisture distribution being weaker and more quickly to balance (Qian et al, 2016).

Moisture movement is an important mechanism of creep and stimulates a great effect from humidity and moisture content on concrete creep. Basic creep is the result of concrete in hydra equilibrium with ambient medium, which is when there is no moisture loss from the concrete specimens. External relative humidity, assuming to be constant for this research study, can increase the magnitude of total deformation for the loaded specimens by enhancing induced shrinkage and consequently influencing the drying creep values. The trend is that a lower relative

humidity environment causes more creeping compared to an environment with higher relative humidity. Specimens completely sealed (100% Relative Humidity) have the lowest creep magnitude since under these conditions, no moisture exchange occurs and, as a result, there is no drying of the specimens (Forth and Ambrose 2018).

With temperature remaining constant, air dried specimens have higher creep strains compared to specimens cured for any duration of time and regardless of how the specimens are cured whether in curing rooms or with burlap. With curing conditions remaining constant, an increase in temperature exhibits higher creep strains on the specimens. Rate of creep increases with decreasing atmosphere humidity, but the relation is not linear at all. Temperature effects on creep are twofold, so an increase in temperature not only increases the creep rate, but also accelerates the hydration (Kennedy 1972).

Both basic and drying creep are also very dependent on the loading age of concrete. Basic creep increases the younger the specimens are loaded. This is because more adsorbed water is still available early on until the process of hydration causes the surface area of gel to decrease within the thickness of the layers of adsorbed water, leaving less available water. Additionally, drying creep decreases with loading age since more water has evaporated prior to loading. The rate of decrease of drying creep is also accelerated in young specimens compared to older specimens because the rate of loss of water is faster in younger specimens (Niyogi, Hsu, and Meyers, 1973).

2.6 Influence of the Steel and Polypropylene Fibers on Creep Performance, Aslani and Nejadi Research Study

Researchers Farhad Aslani and Shami Nejadi conducted an experimental program with shrinkage and creep testing for four mixes: plain SCC, polypropylene fiber SCC, steel SCC, and hybrid SCC. All specimens were kept under maintained stress for at least 364 days within a chamber. Steel fiber reinforced SCC used fibers (Dramix RC-80/60-BN) with length of 60 mm (2.36 in) and had a dosage of 30 kg/m^3, while polypropylene fiber reinforced SCC used fiber types (Synmix 65) with length of 65mm (2.56 in) and had a dosage rate of 5 kg/m^3 (Nejadi and Aslani 2014). The hybrid mix had half the dosages of the other fiber mixes. According to the two researchers, final shrinkage strain values were the following: 870 for plain SCC, 844 for steel fiber SCC, 823 for polypropylene fiber SCC, and 882 for the hybrid mix; and for creep strains, the following values for the mixes were: 1773, 1686, 1997 and 1736 for plain, steel, polypropylene, and hybrid, respectively (Nejadi and Aslani 2014). The creep coefficient of the polypropylene fiber reinforced SCC mix at age 364 days was over 10% higher than the rest of the mixes for the same age. In addition, both the hybrid and steel fiber reinforced mixes had creep coefficients lower than the normal SCC mix. Regarding free shrinkage, the hybrid mix had the highest value followed by the plain SCC, then the steel SCC, then the polypropylene SCC mix.

2.7 Creep Models

Mathematical expressions are created to predict the creep and shrinkage behavior of hardened concrete; and the following models are utilized in this research and discussed in detail in this chapter: ACI209, GL200, Bazant B3, and CEB MC90-99. The stated prediction models are valid for concrete moist cured for at least 1 day and loaded after a day of curing as well as for concretes with mean compressive cylindrical strengths at 28 days between 3000 and 10000 psi. As of now, the models are not calibrated with concrete containing silica fume, fly ash contents more than 30%, or natural pozzolans and

calibration can only be made by testing such concrete compositions. Furthermore, there is no evaluation on calibrating these creep models for self-consolidating concrete mixes fiber-reinforced or not.

The models follow the proceeding testing conditions established to standardize measurements for creep and shrinkage:

1. Creep and Shrinkage are additive and independent of each other

Two sets of the same specimen are subjected to the same curing and environmental conditions with one set not being loaded and the other loaded from 20-40% of the compressive strength. Strains induced from loads are determined by subtracting shrinkage strains from the non-loaded specimens from strains of the loaded specimens (ACI 2008).

2. Linear Aging Model for Creep

Creep is considered approximately proportional to stress provided that the applied load is less than 40% of the compressive strength always. Strain responses may be added using the superposition principle for increasing and decreasing stresses as long as strain reversals are excluded, and temperature and humidity remain constant (ACI 2008).

3. Separation of Creep into Basic and Drying Creep

Basic creep is measured on specimens sealed to prevent the ingression or egression of moisture from or to its environment because it is considered independent of specimen size and shape. Sealed concrete specimens do not have moisture movement into or out of the specimens and any thermal strains are avoided since temperature is constant. Drying creep is defined as the strain remaining after subtracting shrinkage, elastic, and basic creep strains from total strain (ACI 2008).

4. Differential Shrinkage and Creep/Shrinkage and Creep Gradients Are Neglected

Shrinkage strains determined based on ASTMC157/C157M are measure along the longitudinal axis of prismatic specimens. Most of the reported creep and shrinkage data is based on surface measurements

of cylindrical specimens, and so it is assumed that shrinkage and creep strains occur uniformly through the cross section. However, Kristek et al. (2006) confirmed for bridges including a box girder design, the creep analysis which assumes shrinkage and creep to be uniform throughout the cross section is invalid and inaccurate. Rather, the differences in strain gradients decreases as concrete ages (ACI 2008).

5. Stresses due to the curing phase are negligible

Most test programs consider strain measurements to begin once concrete dries. Restrained stresses from swelling and autogenous shrinkage are assumed to be insignificant because of how much larger creep strains are and because of stress relaxation during the early ages of concrete. This assumption leads to overestimated tensile stresses and acts as an appropriate basis for designs when determining deflection and prestress losses (ACI 2008).

Two practical considerations in the models predicting shrinkage and creep are: the mathematical form of their dependency on time and the fitting of the parameters and resulting expressions. Should the mathematical form not accurately describe the creep and shrinkage phenomena, extrapolations may deviate.

2.7.1 ACI 209R-92 Model

Developed by Branson and Christiason in 1971, it is a highly recommended model by the ACI Committee 209 and is very comparable to very recent models. Compared to other models, the ACI 209 is more convenient to handle for matching short-term test data with minimal background knowledge needed. However, it is very limited in accuracy and is empirically based which makes it more difficult to model the shrinkage and creep phenomena. This model only requires the age of concrete once drying starts, age of concrete at loading, curing method, relative humidity, volume-surface ratio, and cement type to function; and only calculates creep coefficient instead of compliance. According to shrinkage data, the ACI209 model overestimates

shrinkage at short drying times and underestimates shrinkage at long drying times, indicating its limitation of its own equation for predicting shrinkage (ACI 2008).

Creep coefficient after time of loading is given with a time ratio multiplied by a value give for ultimate creep coefficient. The average ultimate creep coefficient is 2.35 but tends to be modified with correction factors such as ultimate shrinkage value. Compliance is taken as one plus creep coefficient divided by the modulus of elasticity at time of loading which is based on values of concrete unit weight, cement type, curing conditions and 28-day compressive strength. Because elastic modulus variation with time is not taken into account, it can create problems to the model and limit accuracy (Magnusson 2018).

2.7.2 Bazant-Baweja B3 Model

The B3 model by Bazant and Baweja is based on the mathematical description of more than ten phenomena that influence creep and shrinkage, including asymptotic properties that may be satisfied by a creep and shrinkage model. It is the third major refinement to a series of models developed at Northwestern University in addition to the BP model B3 and BP-KX model B4. Compared to these models, the B3 Model is simpler and more accurate with formulae simplified through sensitivity analysis, the incorporation of a theoretically derived expression instead of an empirical one for drying creep, and calibration by an enlarged data set. The model has been improved so that the coefficient of variation for errors of predicting creep and shrinkage strains are approximately 20% for creep, including basic and drying, and approximately 30% for shrinkage. Model B3 conforms to guidelines formulated by RILEM Committee TC-107 that summarize basic properties of creep and shrinkage (Bazant and Baweja 2001).

B3 uses the compliance function which reduces the risk of errors from using inaccurate values of the modulus of elasticity and separates basic and drying creep (ACI 2008**)**. To work the model, the following factors are needed: age of concrete when drying commences, the age of concrete at loading, aggregate and cement content in concrete, cement type, average compressive strength at 28 days, curing method, relative humidity, shape of specimen, volume-surface ratio, and water content. Additionally, the model may need other input data that is not available at the time, such as specific concrete proportions; so, default values can be considered if this information is not available at the time (ACI 2008).

The B3 model allows for short-term test data extrapolation which is mandatory for highly creep sensitive structures. However, the issues with this update is that it is not possible unless measurements extend into the final stage when the shrinkage curve begins to level off approaching the final value. Before even reaching this stage, it is not possible to determine how much longer the curve rises at a constant slope and when it begins to level off. Therefore, there is no means to determine model parameters unambiguously if data does not reach beyond a certain time (Bazant and Baweja 2001**)**

2.7.3 CEB MC90-99 Model

The CEB model was developed by Muller and Hilsdorf in 1990 and has been revised to include normal and high strength concretes and to separate total shrinkage into autogenous and drying shrinkage portions. The model does not require any information regarding how long curing occurs or the curing conditions, but the duration of drying is considered to have a direct impact and is not neglected. For using the CEB model, the following factors are needed: age of concrete when drying commences, age of concrete at loading, concrete compressive strength at 28 days, relative humidity, volume-surface ratio, and cement type. This method slightly

underestimates shrinkage of most North American concretes and greatly underestimates the shrinkage of concretes with basalt aggregates located in Hawaii, Australia, and New Zealand. This is because European concretes are primarily considered for optimizing the model. The shrinkage prediction is unresponsive to early-age extrapolation using simple linear regression methods, but the creep model is responsive (ACI 2008).

At any given time, the shrinkage strain is divided into autogenous shrinkage, defined as a function of the 28 days mean compressive strength and cement type, and drying shrinkage, defined as the function of 28-day mean compressive strength, cement type, relative humidity, and volume surface ratio. Furthermore, the compliance is separated into instantaneous strain and creep coefficient. The instantaneous strain term is the function of the modulus of elasticity at the time of loading, usually at 28 days, and cement type while creep coefficient is the function of relative humidity, volume-surface ratio, 28 days mean compressive strength and age of concrete at loading. The model offers correction factors for temperatures elevated or reduced and for high stress effects (Magnusson 2018).

2.7.4 GL2000 Model

Developed by Gardner and Lockman in 2000, the GL2000 model is a modified version of the GZ Atlanta 97 model that conforms to ACI209 model guidelines (ACI 2008) The shrinkage strain is the product of a value of ultimate shrinkage strain which is the function of cement type and 28 days mean compressive strength as well as correction factors for humidity and effects of drying time. Compliance for this model is also divided into instantaneous strain term and creep coefficient term. Likewise, instantaneous strain is the function of the modulus of elasticity at the time of loading and creep coefficient has three terms itself which are two terms for basic creep and one for drying creep. All are a function of age of loading, relative humidity, and volume-

surface ratio (Magnusson 2018). The method requires: age of concrete when drying commences, age of concrete at loading, relative humidity, volume-surface ratio, cement type, and concrete compressive strength at 28 days (ACI 2008).

Presented in **Table 2-1** below is a tabular summary of the creep models, highlighting the requirements needed for each model as well as the limits each have for determining shrinkage and creep.

Table 2-1: Overview of Creep Models: Shortcomings and Requirements

Model	ACI 209R-92	B3	CEB	GL2000
Inputs	• Age of concrete (when drying starts), • age at loading • curing method • relative humidity • volume/surface ratio • cement type	• Age of concrete (when drying starts), • age at loading • curing method • relative humidity • volume/surface ratio • Cement type • Aggregate, cement and water content • Shape of specimen • 28 Day Compressive Strength	• Age of concrete (when drying starts) • Age at loading • 28-day compressive strength • Relative humidity • Volume surface ratio • Cement type	• Age of concrete (when drying starts) • Age at loading • Relative humidity • Volume/surface ratio • Cement type • 28 day compressive strength
Shortcomings	• Model overestimates measure shrinkage at low values and underestimates shrinkage at high values. • Compliance function rather insensitive	• Shrinkage equation sensitive to water content	• Underestimates shrinkage of North American concrete and shrinkage model does not respond well to simple linear regression extrapolation	

2.8 Case Study I: Beam Repair in Parking Structure in Sherbrooke, Canada

Self-consolidating concrete was selected as part of the major rehabilitation program of the Webster parking structure in Sherbrooke (Orbe et al 2012). The concrete was to demonstrate its suitability in casting of restricted repair areas and, specifically, the mix was used to repair the bottom and vertical sides of a 6.5-meter-long beam with corrosion damage under the expansion joint. The repair included the use of 3 m^3 of self-consolidating concrete from two 100 mm diameter holes and the concrete had to flow under its own weight along highly restricted sections and around the vertical side to fill the formwork's opposite side. Due to the fact that the repair concrete was used for thin placements over an old base concrete, the maximum drying shrinkage following 28 days of curing (ASTM C 157) was 600 µm/m after 180 days. The binder incorporated 3% silica fume and 20% of Class F fly ash replacement as well as a w/cm ratio of 0.41 to ensure durability. The viscosity modifier admixture was used to enhance cohesiveness and a carboxylic acid water reducer-set retarder was also added to mitigate fluidity loss. A peak temperature of 45 C was measured after 36 hours of age and the ASTM C 666 frost durability coefficient was 90%, showing good frost durability (Orbe et al 2012**)**. Due to difficulties in estimating moisture content of aggregate, the water content of the field concrete was lower than expected, thereby giving the concrete a stiffer consistency but still with adequate air content. The concrete was cast directly into the two holes along the beam through inverted cone hoppers and spread readily along the length of the beam and around the vertical sides. However, at the opposite side of the beam, the concrete did not flow under its own weight through the dense reinforcement. This may had been the result of the lower effective water content. Overall, the mixture had greater compressive strength than anticipated, lower drying shrinkage, and durability that was excellent.

2.9 Case Study II: Application of Steel Fiber Reinforced Self Compacting Concrete

The main components of the steel reinforced SCC mix were CEM I 52.5 R cement, silica fume, limestone filler, and sand and gravel. Superplasticizer used was a policarboxylate-based high range water reducing admixture with a cohesive agent. Steel fiber used was Dramix RC-80/30 BP steel fibers with length 30mm and diameter 0.5mm (Barragan 2004). The concrete was used in the construction of thin walls forming part of a hydraulic channel and no rebar was used in the SFR-SCC walls. Construction time for the walls using this mix was a third of the time needed for conventionally-vibrated concrete and there were no signs of segregation for the SCC mix (Barragan 2004). The study concluded that the steel fiber reinforced self-compacting concrete can adequately self-compact with fiber dosages of up to 40 kg/m^3 (67.4 lb/yd^3). Furthermore, construction time was shortened significantly with the elimination of vibration and rebar reinforcement and consequently, there were considerably cost reductions and errors, making the work environments overall much better when SCC is used.

Chapter III

3. EXPERIMENTAL SETUP

3.1 Introduction

The experimental program includes performing six mixes of self-consolidating concrete with fiber variation, performing immediate and mechanical tests on the concrete samples, and then preparing concrete samples for creep and shrinkage analysis. Immediate tests include slump, j-ring, visual stability index, the T20 test, and air content testing. Mechanical property testing includes determining compressive and tensile splitting strengths, elastic modulus, flexural and permeability values, and creep and shrinkage strain behaviors. Different fiber types and lengths

are added to different mixes with, and high-range water reducer is added until immediate property requirements are met, particularly in slump flow according to ASTM standards.

Most mixes have only one type of fiber involved, either steel fibers of 1.5'', polypropylene fibers of 1.5'', or polypropylene fibers of 2''. There are two hybrid mixes: one that combines both the steel and polypropylene fibers of 1.5'' length and one that includes micro polypropylene fibers of ¾'' length and macro polypropylene fibers of 1.5'' length. The fact that fibers reduce flow of concrete is countered by the fact that the following mixes are self-consolidating, which thrive in ensuring workability of concrete especially for dense reinforced areas. Immediate concrete properties are observed and recorded to acquire a more in-depth analysis of how the fibers influence flow compared to a control mix. Onward, mechanical properties are recorded over a period of 28 days to observe the progression of compressive and tensile strength, elastic modulus, and free shrinkage and how each fiber type affects these properties. Finally, each mix is tested for creep behavior over a standard period of 1 year within a controlled environment using standard creep loading rigs. Grade 120 Slag is utilized throughout the process as well as water reducing agents and air entraining admixtures to satisfy standards.

3.2 Material Properties

All materials are made readily available within New Jersey that would be most accessible to companies and agencies that would use the same material locally. Most of the cementitious materials come from different suppliers within New Jersey while all aggregates, fine and coarse, and Portland Cement are acquired from Clayton Concrete in Edison, New Jersey. **Table 3-1** summarizes materials and respective suppliers as well as any specific details necessary to acknowledge.

Table 3-1: Materials and Suppliers

Material	Type(s)	Supplier(s)
Cement	Portland Type I Cement	Clayton Concrete
GGBFS	Grade 120	Holcim LaFarge
Fine Aggregate	Concrete Sand	Clayton Concrete
Coarse Aggregate	#8 (3/8'') Granite	Clayton Concrete
Water Reducer	Plastol 5000	Euclid Chemical
Air Entraining Agent	AEA 92S	Euclid Chemical
Polypropylene Fibers	1.5'' (Tuf-Strand MaxTen) Synthetic Macro 2'' (Tuf-Strand SF) Synthetic Macro 0.75'' (PSI-Fiberstrand 100) Monofilament Micro	Euclid Chemical
Steel Fibers	1.5'' Crimped	Euclid Chemical

The specific HRWR agent used in this research is the Euclid Chemical Company's Plastol 5000. It is a ready to use polycarboxylate based admixture that increases early and ultimate strength of concrete while also reducing the quantity of water as needed in SCC mixes. Plastol 5000 complies with the requirements of ASTM C 494, Type A & F admixtures as well as ASTM C 1017 Type I Admixtures and is compatible with most admixtures such as air-entraining agents, other water-reducers, viscosity modifiers, and micro silica ("Plastol 5000: High Range Water Reducing Admixture").

The air entrainment agent to be used for this research is Eucon AEA-92S, an admixture formulated and manufactured under rigid control. The solution is combined from synthetic organic chemicals allowing compatibility with several different concrete mixes containing calcium chloride, water reducing admixtures, or high range water reducers. It provides all the required benefits needed from an AEA agent as well as compliance to ASTM Specs. C260, AASHTO Specs. M 154, and ANSI/NSF STD 61 regulation ("Eucon AEA92 Air Entraining Agent for Concrete").

Figure 3-1 presents polypropylene fibers, a type of synthetic fiber emphasized in this research. They are manufactured in small bundles that open into individual fibers as they shear apart from each other during the mixing procedure.

Figure 3-1: Polypropylene Fibers of Length 1.5'', 2.0'', and 0.75''

As shown in **Figure 3-2**, steel fibers are distinguished based on their physical manipulation compared to polypropylene fibers. The steel fiber in this case, is crimped shaped.

Figure 3-2: Steel Fibers, Crimped Shaped and 1.5'' Length

The properties to all fibers used in this research are outlined in **Table 3-2.**

Table 3-2: Properties of Fibers

Material	1.5'' Macro Polypropylene	2.0'' Macro Polypropylene	1.5'' Steel	0.75'' Micro Polypropylene
Specific Gravity	0.91	0.92	7.7	0.91
Melting Point (°F)	320	320	2500	320
Aspect Ratio	79	74	34	- - -
Typical Dosage (lb/yd^3	3 to 5	3 to 20	25 to 100	1.0

3.3 Mix Proportions

Two sets of mixes are performed for each mix type: One strictly for mechanical and immediate property testing results only and another for making creep cylinders and ensuring consistency with results. The mix proportions creep analysis mixes are summarized in **Table 3-3** below.

Table 3-3: All Mix Proportions – Creep Rigging Cylinders

Mix	Control	PPE1.5''	PPE2''	ST1.5''	HYB-1	HYB-2
Cement, Type 1 (lb/cy)	439	439	439	439	439	439
Slag, Grade 120 (lb/cy)	236	236	236	236	236	236
Total Cement (lb/cy)	675	675	675	675	675	675
W/C Ratio	0.400	0.406	0.402	0.401	.37	.413
#8 Rock Aggregate (lb/cy)	1436	1436	1436	1436	1425	1425
Sand (lb/cy)	1447	1447	1447	1447	1485	1453
High-Range Water Reducer (oz/cwt)	14.0	7.0	9.0	6.0	12.0	12.0
Air Entrainment Agent (oz/cwt)	2.0	2.0	2.0	2.0	2.0	2.0
Fiber Type	None	Macro PPE Fibers	Macro PPE Fibers	Steel Fibers	Macro PPE and Steel Fibers	Micro and Macro PPE Fibers
Fiber Length	None	1.5''	2''	1.5''	1.5''	0.75'' and 1.5''
Percent by Weight	0%	0.130%	0.130%	0.652%	0.065% And 0.326%	0.0131% and 0.0653 %

Percent by Volume	0%	0.320%	0.320%	0.193%	0.163% and 0.0965%	0.160% and 0.03%

Table 3-4 summarizes mix proportions for samples made primarily for mechanical and immediate testing and shrinkage data acquirement over a period of 28 days.

Table 3-4: All Mix Proportions – Mechanical Property and Shrinkage Testing

Mix	Control	PPE1.5''	PPE2''	ST1.5''	HYB-1	HYB-2
Cement, Type 1 (lb/cy)	439	439	439	439	439	439
Slag, Grade 120 (lb/cy)	236	236	236	236	236	236
Total Cement (lb/cy)	675	675	675	675	675	675
W/C Ratio	0.4	0.4	0.4	0.4	0.4	0.4
#8 Rock Aggregate (lb/cy)	1436	1436	1436	1436	1436	1436
Sand (lb/cy)	1447	1447	1447	1447	1447	1447
High-Range Water Reducer (oz/cwt)	8	10	10	10	12	12
Air Entrainment Agent (oz/cwt)	2.0	2.0	2.0	2.0	2.0	2.0
Fiber Type	None	Macro PPE Fibers	Macro PPE Fibers	Steel Fibers	Macro PPE and Steel Fibers	Micro and Macro PPE Fibers
Fiber Length	None	1.5''	2''	1.5''	1.5''	0.75'' and 1.5''
Percent by Weight	0%	0.130%	0.130%	0.652%	0.065% And 0.326%	0.0131% and 0.0653 %
Percent by Volume	0%	0.320%	0.320%	0.193%	0.163% and 0.0965%	0.160% and 0.03%

For all mix proportions, total cementitious material is divided into 35% Grade 120 blast furnace slag and 65% Type I Portland Cement. A water/cementitious ratio of 0.400 is maintained and approximately equal amounts of coarse and fine aggregates are used in the mixes for a 1:1 ratio. High-range water reducer quantity is manipulated based on the immediate results of the

slump for fresh concrete during the mixing procedure. Air entraining agent quantities are kept at a constant amount for all mixes.

Fiber quantity per cubic yard only varies based on the type of fiber used for a specific mix. Due to its high density, there is a greater weight per cubic yard for steel fibers compared to polypropylene fibers. With the addition of the fibers, workability of the fresh concrete reduces and may not often pass slump testing. In response, different amounts of HRWR are added for each mix until workability requirements are met especially when performing J-ring testing.

3.4 Fabricating Creep Sample Specimens

Before mixing occurs, 6'' x 12'' concrete cylinders are modified for creep testing. As seen from **Figure 3-3**, ¼'' bolts protrude out of the sides of the cylinder at 120-degree angles.

Figure 3-3: 6'' x 12'' Cylinder Modified for Creep Testing

The purpose of this is to allow placement of the vibrating wire strain gages onto the sides of the concrete specimen once they are cured and ready at 28 days. Nuts of ¼'' diameter are placed both inside and outside the bolts to ensure that they are straight and always stiff during the

mixing procedure. During the demolding procedure, the molds are sliced apart and discarded, and the bolts protrude out of the concrete at 120-degree angles with enough length to accommodate for the strain gages.

3.5 Mixing, Immediate Testing, and Sampling

Mixing and casting is performed based on ASTM 19 and procedures for all aspects of mixing and testing are discussed in the following section in chronological order.

3.5.1 Mixing

Figure 3-4 presents the electric mixer used for all mixes. It can hold 6 cubic foot of concrete at a time and has no major issue with its capacity or function as of now.

Figure 3-4: Electric Mixer Within the Lab

Prior to every mix, the appropriate amount of batching material is pre-batched into several clean buckets, labeled, and organized as to increase productivity of the mixing process

itself. Moisture content is performed three hours before every mix and adjustments are made to the fine and coarse aggregates as needed to prevent water/cement ratio issues. Because both sets of mix proportions are less than 6 cubic foot, every mix is usually done in a single session.

Mixing of the concrete follows ASTM C192 standards. Prior to beginning the mixer, coarse aggregate and some of the water mixed with air entraining agent are added. Once the mixer starts, fine aggregate, cement and water are added while the mixer runs. When all ingredients are added, the mixer is left to rotate for 3 minutes followed by a 3-minute resting period followed by a 2-minute mixing period. The mixer is covered to prevent evaporation during resting and high range water reducing agent is added right after all ingredients are mixes effectively.

3.5.2 Slump Flow Test (ASTM C1611), T20, & Visual Stability Index (VSI)

Due to the nature of self-consolidating concrete, standard slump test protocol (ASTM C134) is not applicable. ASTM C1611 standards utilize the same equipment but in a different manner; instead, the slump cone is flipped upside down and concrete casted into the cone is not rodded in layers at all. Once the inverted slump cone is filled, it is lifted gradually to shoulder height in the matter of 3 seconds, and the horizontal diameter of the concrete slump is measured rather than the vertical height. To determine the T20 value, a timer is used to measure elapsed time between raising the cone and the point at which the slump flow passes the 20-inch diameter circle marked on the base plate. Currently, there is no implemented required T20 value for SCC mixes to pass standards. **Figure 3-5 and 3-6** visually demonstrate how the slump test is prepared for self-consolidating concrete mixes and how the concrete flows up to the 20-inch diameter in the horizontal direction.

Figure 3-5: ASTM C1611 Slump Test with Board

Figure 3-6: SCC Slump Flow on the Board

Once the concrete seizes to flow, the largest diameter of the resulting flow is recorded; then the diameter perpendicular to this is also recorded and the two measurements are averaged. Generally, an average diameter of 18 inches is recommended to pass the initial slump flow test for self-consolidating concrete mixes. Additionally, the flow is observed for any possible

bleeding or segregation issues based on the amount of water leaking from the side of the concrete flow; and this bleeding is measure with the VSI index. A VSI index ranges from 0 to 3 with 0 meaning no evidence of bleeding in the mix and 3 being a major indication that the concrete is unstable. A VSI index of 1 tends to be the acceptable limit for passing since it only signifies slight bleeding issues but acceptable stability of the concrete for use. A VSI index of 2 or more concludes that the mix does not pass since the bleeding is too excessive as the "halo" around the concrete exceeds half an inch thickness and the aggregate is visibly segregating.

3.5.3 J-Ring Testing (ASTM C1621)

Following slump flow, T20, and VSI index testing of the mix, J-Ring testing comes next for determining the passing ability of self-consolidating concrete through dense reinforcement. The same equipment from slump flow testing is used only now a large metal ring circles around the slump cone as shown in **Figure 3-7.**

Figure 3-7: SCC J-Ring Test Set Up

The device is 12 inches in diameter and holds 16 circular bars around it to simulate practical dense reinforcement in the construction industry. The same protocol is followed as with slump flow testing but T20 and VSI testing is now disregarded. Only the average of the largest diameter and perpendicular diameter is noted and compared to the average diameter of the slump flow testing. The purpose is observing the difference between the two numbers and determining how much blockage occurs due to the reinforcement. A difference of no more than 1 inch is ideal since it indicates no signs of blockage, while a difference between 1 and 2 inches indicates minimal blockage issues happening. A difference exceeding 2 inches signifies that the mix is excessively blocked and does not pass the J-ring testing.

3.5.4 Air Content Test Via Pressure Method

Figure 3-8 shows the Type B pressure air meter used for determining air content of the concrete mixes for this research study.

Figure 3-8: ASTM C231 Type B Pressure Air Meter

The test is performed while J-Ring testing occurs and passes when the concrete air percentage is within a range of 4 to 7%.

3.5.5 Sampling and Casting Procedure

Once a mix passes fresh concrete property testing, casting follows. Samples include three free shrinkage prisms measuring 4 x 4 x 10 inches and four rectangular prisms measuring 3 x 3 x 12 inches for flexural testing. All specimens are measured for wet shrinkage as they are placed within the curing room for the first 14 days. Additionally, approximately 35 to 40 4 x 8 cylinders are made for testing the mix for mechanical properties over a period of 28 days. Moreover, 10 6 x 12 cylinders are made for the creep testing at 28 days. A quick set up of the samples is shown in **Figure 3-9**.

Figure 3-9: Samples Prepared for Casting

For a batch not involving creep samples, no 6 x 12 samples are used, and only 4 x 8 cylinders and shrinkage prisms are utilized.

3.5.6 Curing and Storage

Both sets of samples are cured and stored in the same manner. Once casting is complete, all samples are placed within the environmental chamber for the first 24 hours. Afterwards, the demolding process occurs and most samples are placed within the curing room until the 14th day of curing. Creep samples are placed in water baths within the curing room to maximize humidity conditions until ready for use. **Figure 3-10** presents the curing room itself and the location of the water baths containing the concrete samples.

Figure 3-10: Curing Room

3.6 Mechanical Property Testing

Mechanical property testing is performed 1, 3, 7, 14, and 28 days after mixing with the 6 x 12 cylinders tested only at 28 days for compressive and modulus testing only.

3.6.1 Compressive Strength Test (ASTM C39)

Figure 3-11 presents the set up for compressive strength testing of a 4 x 8 concrete specimen using a compression machine with a capacity of 1,000,000 lbs.

Figure 3-11: Compressive Strength Test

Compressive testing is done using either sulfur capping material for the top and bottom of the specimen or by using steel capping devices, both meant for ensuring a flat and level surface on the specimen so that loading is uniform and prevents eccentricity during loading. **Figure 3-12 and Figure 3-13** present the sulfur and steel capping devices and how they are placed on the specimens for testing.

Figure 3-12: Sulfur Caps on the Concrete Specimens

Figure 3-13: Steel Caps on the Concrete Specimens

Once capped, a specimen is loaded until failure indicated by a major breakthrough in the cylinder usually originating from shear across the specimen. Three cylinders are tested for accuracy and consistent results.

3.6.2 Tensile Splitting Test (ASTM C496)

Figure 3-14 presents the setup of tension testing on a concrete specimen using the same machine for compression testing.

Figure 3-14: Tensile Strength Testing Setup

Each specimen is placed horizontally on its side on top of a thick rectangular plate. The cylinder is tested until failure indicated by a very visible crack along the center. Three specimens are tested for accuracy and consistent results.

3.6.3 Elastic Modulus Testing (ASTM C469)

Figure 3-15 presents the proper setup for elastic modulus testing of a concrete specimen using the same compression machine.

Figure 3-15: Elastic Modulus Testing Setup

Data acquired from compression testing from the same samples of the mix are used to determine the max elastic loading range. Cylinders are loaded at most 40% of their compressive strength based on the average of the three cylinders tested for compression. Strain readings depend on the elastic load but always follow the protocol of having 6 strain readings for evenly spaced out load readings. Two cylinders are tested twice for consistency.

3.6.4 Free Shrinkage Testing (ASTM C157)

Free shrinkage measurements are taken at specific intervals depending on the time after curing and type of shrinkage being monitored. Specimens initially in wet conditions are measured only 3 times until 14 days when they are removed from the curing room and placed in dry conditions. Afterwards, they are measured twice per week until 28 days. Shrinkage samples are placed in an environment with a controlled temperature and humidity to reduced variability in the data due to unforeseen and uncontrollable factors such as thermal expansion. **Figure 3-16** shows the shrinkage device used in this research study

Figure 3-16: Free Shrinkage Testing Setup

As seen, a rod is used for reference for length comparison. Each prism is tested 3 times or until readings are consistent to each other and all prisms are tested together whenever possible to improve accuracy.

3.6.5 Flexural Testing (ASTM C78-02)

Flexural testing is performed on 14 and 28-day testing periods for all mixes. **Figure 3-17** shows the setup of the flexural testing of the specimens. The procedure follows ASTM C78-02 which is third point loading for a beam.

Figure 3-17: Flexural Testing Apparatus

3.6.6 Rapid Chloride Permeability Testing (ASTM 1202)

RCPT testing is performed on 28 days testing as well and **Figure 3-18** presents how the concrete specimens are used to collect data.

Figure 3-18: Rapid Chloride Permeability Testing

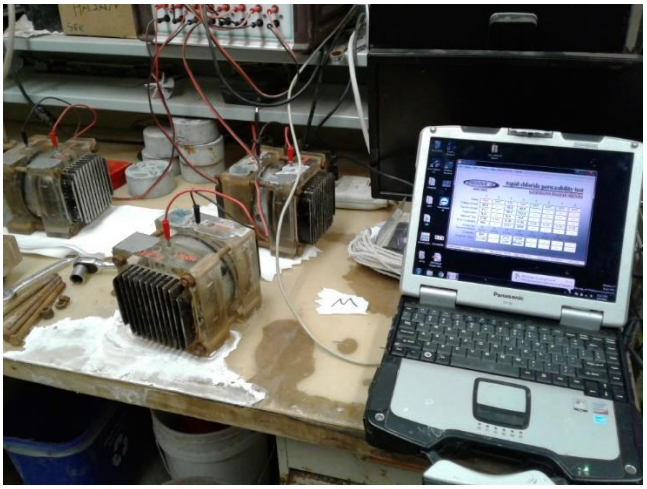

3.7 Environment of Creep Chamber

The chamber is meant to maintain an environment of constant temperature and humidity, approximately 24.0 degrees Celsius and a humidity of 50%. Henceforth, the environmental chamber holds free shrinkage samples, creep samples, and all concrete samples older than 14 days, all of which are heavily influenced by temperature and humidity. The chamber itself is made of insulated aluminum wall, and temperature and humidity are controlled with a digital control unit located outside the room next to the entrance as seen in **Figure 3-19**.

Figure 3-19: Digital Control Unit for Environmental Chamber

Within the room are heaters and freezers that occupy one side of the wall and control the temperature. The chamber currently holds 16 creep rigs as shown in **Figure 3-20**.

Figure 3-20: Creep Rigs within Environmental Chamber

3.8 Creep and Shrinkage Testing Procedure

3.8.1 Creep Loading Rig Set-Up

To proceed with the creep testing of concrete samples, the following creep loading rig is utilized as shown in **Figure 3-21**.

Figure 3-21: Creep Loading Rig

Each rig is designed for three 6 x 12 in. creep specimens as well as 2 4 x 6 in. smaller specimens of the same concrete mix. The rig uses two 20 x 20 x 2 in. large steel plates, two 15 x 15 x 15 in. smaller steel plates, five double coiled springs, and four threaded rods. The large steel plates hold the coiled springs and functions such that one plate is fixed and unable to move while the other is free to move up and down. The purpose is to apply the required compression load on the concrete specimen "tower" by manipulating the free moving steel plate and maintaining the applied load through large steel nuts threaded into the steel rods. The double-coiled springs are capable of 200 kips of loading. On the bottom of the "concrete tower" lies a Geokon load cell as seen in **Figure 3-22**.

Figure 3-22: Geokon Load Cell Monitoring Load of Rig

The load cell shows the maintained load of the rig over the period of testing through the P3 Strain Indicator and determines the amount of creep relaxation occurring through load reduction over time. On the very bottom of the rig itself are the smaller steel plates which provide space for the hydraulic jack pump to be used to induce the load on the rig. As seen on **Figure 23**, the jack must be centered and pushes the coiled springs to stimulate the load on the specimen.

Figure 3-23: Hydraulic Jack Pump

3.8.2 Creep Testing

First, (10) 6 x 12 concrete specimens are removed from the curing room 28 days after being demolded. Beforehand, 5 or 6 of the specimens have been modified for creep testing, and those same specimens are sulfur capped with 3 being meant for creep testing and 2 for free shrinkage data collection. Another 3 not modified for creep testing are sulfur capped and tested for calculating the average concrete compressive strength (f'c). The purpose is to acquire 35% of this average as the desired loading used for creep testing. One specimen, additionally, is cut into 3 pieces so that 2 of the pieces are size 4 x 6 in.

Next, all appropriate concrete specimens are aligned on a creep rig with the load cell having a 12-inch diameter steel plate between itself and the first concrete specimen to better distribute the upcoming load. Once the concrete specimen is set and centered, the top plate is adjusted to be in contact with the top of the concrete specimen, and the jack is placed underneath the rig to prepare for loading. When all is finished, nuts on the bottom of the top plate and on the top of the

bottom plate are loosened to allow space for compression. The load is monitored through the Geokon Load Cell and loading may commence once the jack is centered properly.

Finally, once the load is reached, the bolts on the bottom of the bottom plate must be tightened as uniformly as possible to prevent load eccentricity and the process is complete. Over time, creep relaxation occurs in which the load gradually decreases. Therefore, the load must be adjusted periodically to prevent excessive loss of load magnitude due to this phenomenon. Less than 2% of the total applied load at the beginning is the recommended range.

3.8.3 Data Collection System

All creep and shrinkage strain data are collected through vibrating wire strain gages which have an initial reading around 3500 micro strains before loading. As shown in the image on the left in **Figure 3-24**, the gauges are installed 120 degrees from each other and the average strain readings on a specimen is used for the total strain calculations. The right image presents the customized mold that is used for creating the customized 6 x 12 specimens for installation of the gauges.

Figure 3-24: Vibrating Wire Strain Gages on the Side of a Concrete Specimen

In total, 15 gages are installed for 1 set of concrete specimens: 9 for the creep specimens and 6 for the free shrinkage specimens which are unloaded and adjacent to the rig. Averages for each specimen are determined and those averages result to the final values of total creep and shrinkage strain. During creep testing, some values are disregarded if they are deemed unreasonable or show signs of malfunction to keep consistency. Since 6 total rigs are used for this research, the project is very data intensive and requires constant monitoring of the rigs. As a result, the Campbell Scientific Loggernet System, involving one CR1000 and several AM16/32s multiplexers and AVW200s, is used. As shown in **Figure 3-25**, the data logger system is placed within a white contained latched onto the wall and may be directly connected to a computer or laptop through a USB Cable. Data can be exported to Microsoft Excel or any other data processing programs for convenience.

Figure 3-25: Creep Research Datalogger System

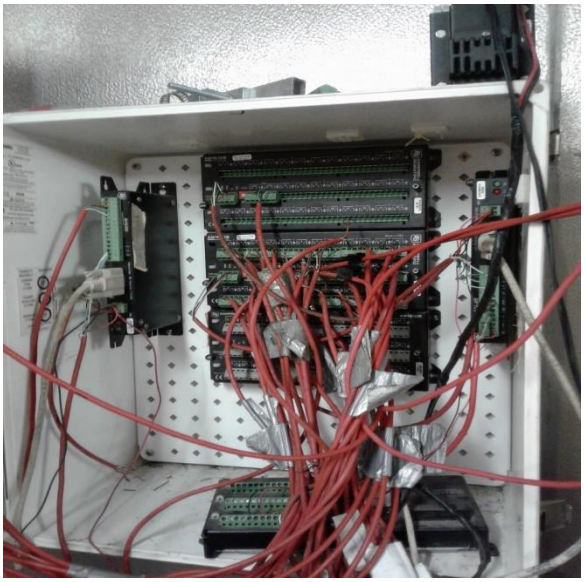

CHAPTER IV

4. RESULTS AND ANALYSIS

4.1 Introduction

The following chapter includes all test results related to fresh and mechanical property, creep and shrinkage testing results of the concrete mixes evaluated.

4.2 Fresh Concrete Test Results

Results of slump flow, j-ring slump flow, T20, visual stability index, and air content percentage are presented in **Table 4-1**. Because some mixes did not meet standards with the initial dosage of superplasticizer, an additional amount was added and final amounts are tabulated with the final value of slump flow and j-ring flow.

Table 4-1: Immediate Property Testing Results

Mix	T20 (s)	VSI	Air (%)	Super P Added (Oz)	Slump Average	Jring Average	Slump – Jring Average
CONTROL	6.4	1	6	8	20	18.625	1.375
PPE1.5	11	1	6	10	20.75	19	1.75
PPE2	14	1	5	10	17	15	2
ST1.5	7.2	0	5.5	10	22.75	21	1.75
HYB-1	9.22	1	6.5	12	21.5	19.825	1.675
HYB-2	9.83	1	6.2	12	24.5	22.5	2

4.2.1 T20

T20 values represent the viscosity of a self-consolidating mix and should never exceed 20 seconds. The inclusion of the 1.5’’ macro polypropylene fiber greatly increases the viscosity of the mix even with the addition of more superplasticizer admixture. On the other hand, mixes

with steel fibers included have a shorter T20 time compared to mixes with 1.5'' macro polypropylene included. Mix with 2'' macro polypropylene has the highest T20 value while having the same quantity of HRWR added, highlighting the strong impact that the fiber type has on the viscosity of self-consolidating concrete. The inclusion of the micro fibers reduces viscosity of the mix compared to steel fibers as shown between the two hybrid mixes.

4.2.2 VSI

All mixes showed trivial amounts of segregation and bleeding with the ST1.5'' mix showing no signs of segregation.

4.2.3 Slump Flow

It is recommended for the slump flow to reach at least 18'' diameter for self-consolidating concrete. Macro polypropylene fibers of 2'' length included at a dosage of 5lb/yd^3 causes a greater reduction in slump flow than macro fibers of 1.5''; the reduction is roughly 18% more for the same dosage and same amount of HRWR admixture added for each mix. On the other hand, the steel and micro polypropylene fibers have little influence to the slump flow compared to both macro polypropylene fibers even when they are combined in hybrid mixes.

4.2.4 J-Ring

The difference between the slump flow and J-ring value should not exceed 2'', marking the mix's ability to compact into dense reinforcement well enough for application. Once again, the influence of 2'' macro fibers is stronger in reducing workability compared to 1.5'' macro fibers as the difference for the PPE2'' mix nearly exceeds 2 inches. Furthermore, the 0.75'' micro fibers shows a greater influence in reducing slump flow with the presence of dense reinforcement.

4.2.5 Air Content

All mixes are within range between 4 to 7% by volume air content to satisfy standards and ensure that the mixes do not lose efficiency for freeze and thaw cycles in application.

4.3 Compressive, Tensile, and Modulus Test Results

Results for compressive strength, tensile strength, and modulus of elasticity for 1,3,7,14, and 28-day testing are presented in **Table 4-2 to 4-4 and Figures 4-1 to 4-3**. Values are presented in pounds per square inch (psi). A total of 4 to 5 cylindrical samples are tested for the appropriate day and are capped using sulfur capping compound. The cylinders tested for modulus of elasticity are also used for tensile strength results since they do not reach inelasticity during testing of elastic modulus.

Table 4-2: Compressive Strength (Psi) of Mixes over 28 Days

Days	Control	PPE1.5	PPE2	ST1.5	HYB1	HYB2
1	2866	1850	1433	1557	2516	1831
3	3822	2344	1895	2038	2659	2229
7	4754	3697	2588	2508	2787	3129
14	5449	4016	3105	3376	2988	3344
28	6365	4772	3710	3543	3822	4220

Figure 4-1: Compressive Strength of Mixes

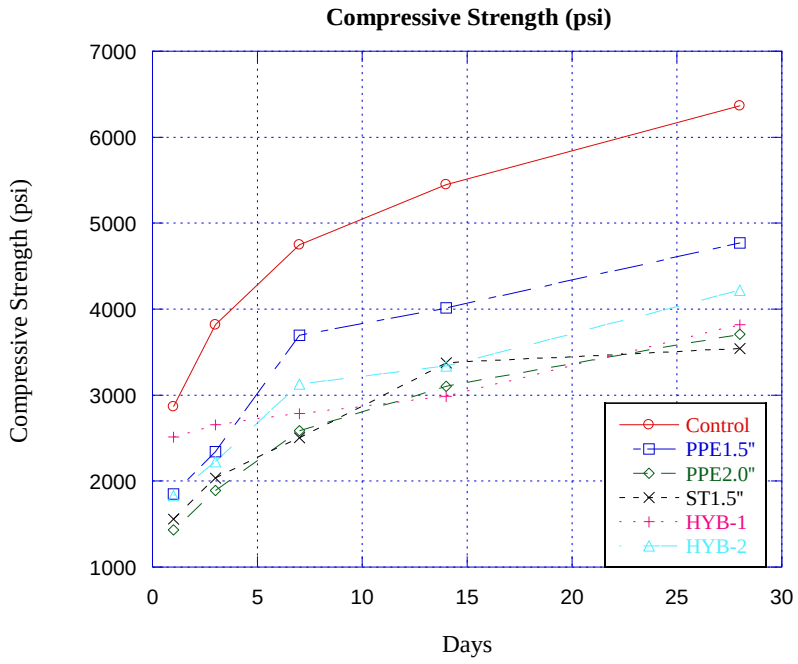

As presented, addition of steel fibers causes an overall decrease in compressive strength by about 44% and the addition of polypropylene fibers for 1.5'' and 2.0'' length cause reduction by about 25% and 42%, respectively. Between the two hybrid fiber mixes, the hybrid combination of steel and polypropylene fibers causes a greater reduction of 40% compared to the hybrid combination of polypropylene macro and micro fibers which is a 34% reduction.

Hence, the addition of the crimped steel 1.5'' fibers causes more reduction to compressive strength than polypropylene fibers for the self-consolidating mixes. Meanwhile, the polypropylene 1.5'' fibers cause the least reduction in strength.

Table 4-3: Tensile Strength (Psi) of Mixes Over 28 Days

Days	Control	PPE1.5	PPE2	ST1.5	HYB1	HYB2
1	260	348	256	314	290	278
3	315	503	364	402	465	334
7	346	636	462	474	485	384
14	394	676	542	494	520	408
28	416	644	520	520	636	388

Figure 4-2: Tensile Strength of Mixes

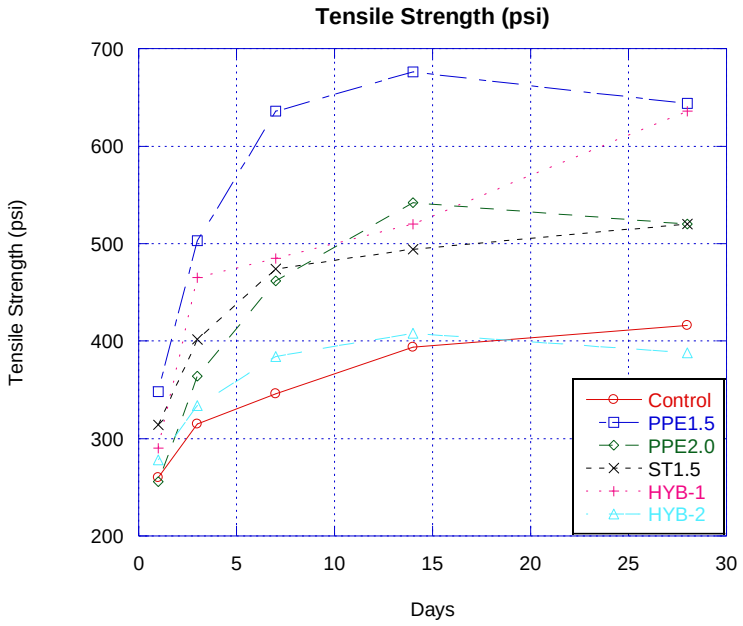

As presented, both the polypropylene 1.5'' fibers and the HYB-1 fiber mix cause the greatest increase in tensile strength by more than 50%. The polypropylene 2'' fiber mix and steel 1.5' mix cause an increase of about 25% by 28 days and the hybrid combination of macro and micro fibers, on the contrary, causes a decrease in tensile strength by 7%.

Hence, the addition of polypropylene fibers of 1.5'' provides the most influence in enhancing tensile strength of SCC mixes, while the hybrid fiber combination of macro and micro polypropylene fibers does not increase tensile strength at all but rather reduces it, concluding that the micro fibers may not be advantageous for tensile strength.

Table 4-4: Modulus of Elasticity (Psi) of Mixes Over 28 Days

Days	Control	PPE1.5	PPE2	ST1.5	HYB1	HYB 2
1	3757	2379	2496	2508	3184	3067
3	4262	2815	2612	2848	4074	3157
7	5983	3223	2802	2801	3652	3403
14	5728	3534	3196	3187	3693	3499

28	5377	3334	2587	3582	3741	3304

Figure 4-3: Modulus of Elasticity (psi) of Mixes

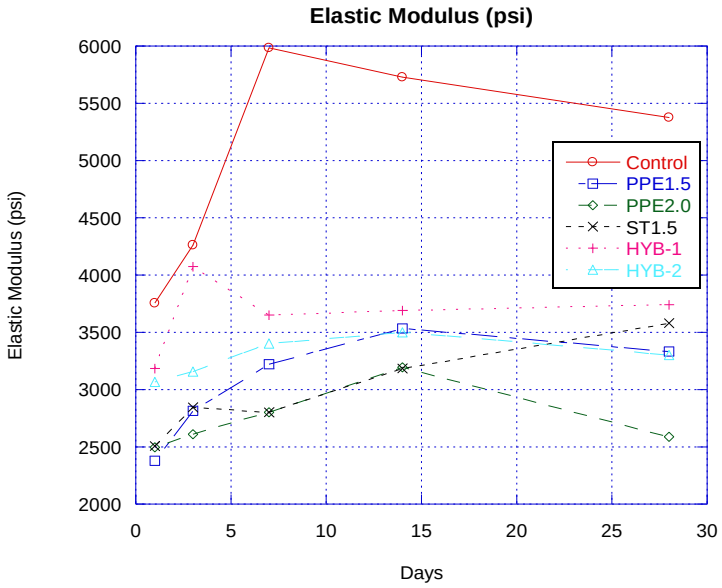

As presented with the data, polypropylene 2'' fibers cause the most decrease in modulus by almost half while HYB-1 causes the least reduction by 33%. Compared to polypropylene fibers, steel fibers have higher modulus of elasticity values by 28 days. Hence, polypropylene and steel 1.5'' fibers are most effective in preventing excessive reduction in modulus for SCC mixes.

4.4 Free Shrinkage

Free shrinkage measurements over a 28-day period are presented in **Figure 4-4** for all mixes.

Figure 4-4: Free Shrinkage Behavior over 28-Day for All Mixes

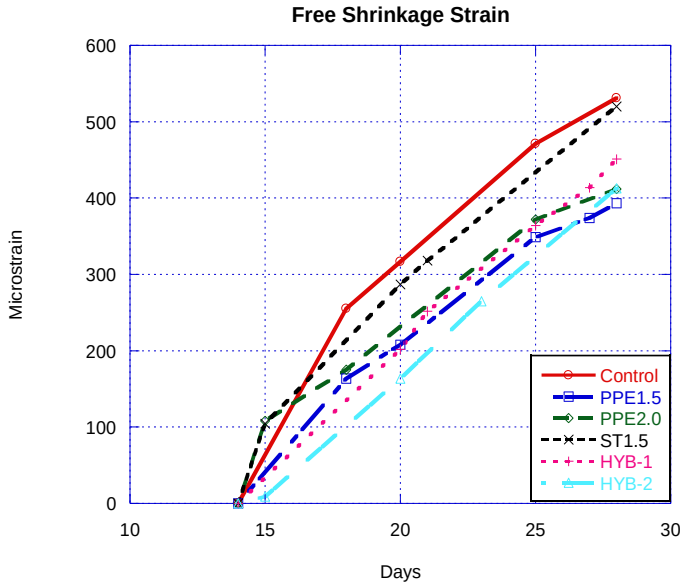

Polypropylene 1.5'' fibers cause the highest reduction in shrinkage compared to all other fibers while steel fibers have very little influence to reducing shrinkage. The presence of micro fibers provides more influence in reducing shrinkage compared to steel fibers as shown with the hybrid mixes. Hence, polypropylene fibers are more encouraged in preventing excessive shrinkage to self-consolidating concrete than steel fibers and micro fibers are more recommended for shrinkage purposes than steel fibers.

4.5 Flexural Testing, and Rapid Chloride Permeability Testing Results

Table 4-5 displays 28-day rapid chloride permeability testing for all mixes. Two cylinders are used for RCPT testing. All results are the average of the two samples.

Table 4-5: Rapid Chloride Permeability Testing Results

Day	Control	PPE1.5''	PPE2''	ST1.5''	HYB-1	HYB-2
28	1729	1823	2403	1722	2567	1774

As presented, steel fibers are able to lower the value of permeability while polypropylene fibers of 2'' cause increased permeability by almost 40%. Between the two hybrid mixes, the presence of micro fibers is more effective in reducing permeability than steel fibers. Hence, micro polypropylene and steel fibers are more encouraging in reducing permeability of SCC mixes

Table 4-6 displays 14 day and 28 day results for flexural testing for all mixes. Two 3'' x 3'' x 12'' samples are used for each testing day and the average max load as well as moment capacity are shown.

Table 4-6: Flexural Test Results (Max Load in lbs)

Mix	14 Day	28 Day	Change
Control	2176	1857	-15%
Polypropylene 1.5''	2140	1999	-6.6%
Polypropylene 2''	1673	1563	-6.6%
Steel 1.5''	1803	1389	-23%
Hybrid 1	1740	1660	-4.6%
Hybrid 2	2051	1718	-16%

Both the macro polypropylene fibers cause the least reduction in flexural strength compared to steel fibers. Furthermore, the presence of micro fibers causes a greater reduction than steel fibers as shown with the hybrid mix results. Polypropylene 1.5'' fibers have comparable strength with non-fiber-reinforced SCC mixes at 14 days and, furthermore, have the least reduction after 28 days of concrete age. Both the steel and micro fibers do not have as much initial strength at 14 days and also cause more reduction by 28 day of age, thereby confirming the effectiveness of macro polypropylene fibers for flexural behavior of self-consolidating concrete mixes.

4.6 Creep Shrinkage and Specific Creep Results

4.6.1 Introduction

Results for creep and shrinkage strain are organized based on mix. Total strain, free shrinkage strain, and creep strain graphical data from the sensors, by this order, are presented as well as the loading variation recorded from the Geokon load cell for each mix. After discussion of each mix, the creep and specific creep data are compared based on the influence of the fibers.

4.6.2 Control Mix

Figure 4-5 to 4-8 present VWSG data from the concrete specimens being tested for creep. Sensors 1 to 9 record for concrete specimens that are under load and contain creep shrinkage, while sensors 10-15 record only free shrinkage data.

Figure 4-5: Top Creep Cylinder, Sensors 1 – 3 (Control)

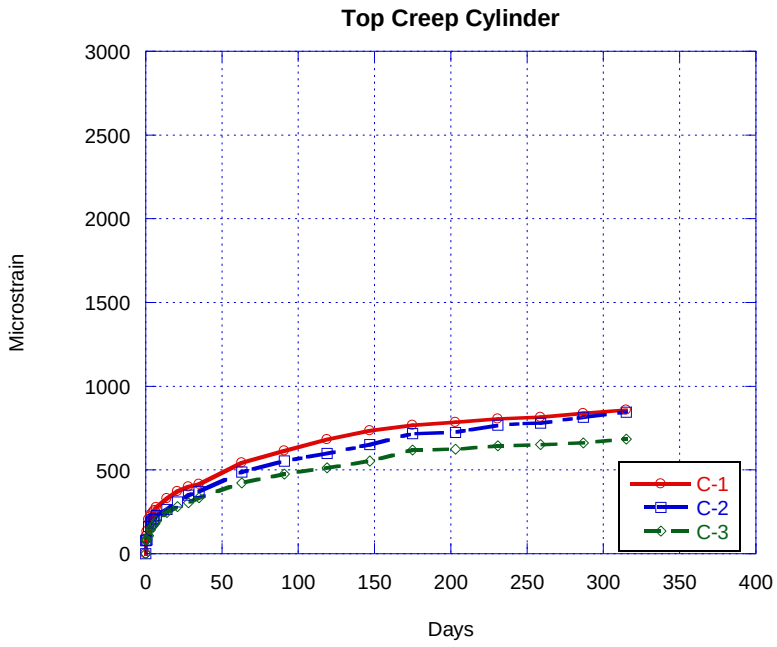

Figure 4-6: Middle Creep Cylinder, Sensors 4 – 6 (Control)

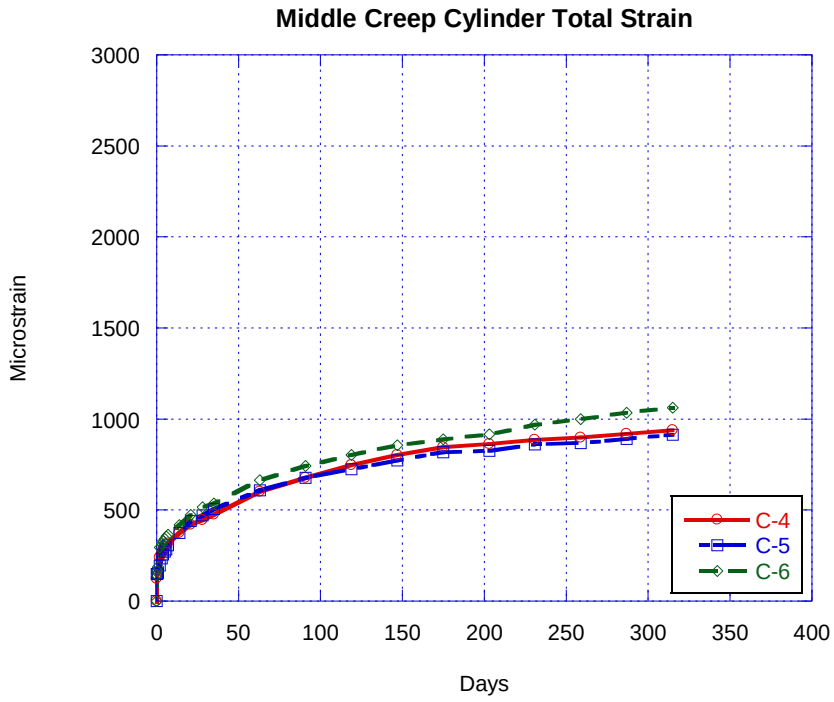

Figure 4-7: Bottom Creep Cylinder, Sensors 7 – 9 (Control)

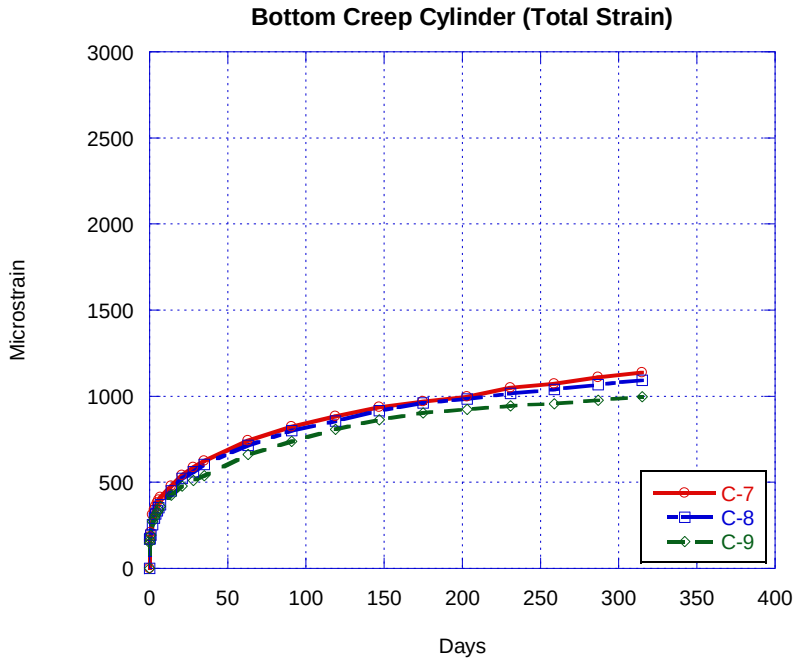

Figure 4-8: Free Shrinkage Cylinders, Sensors 10 – 15 (Control)

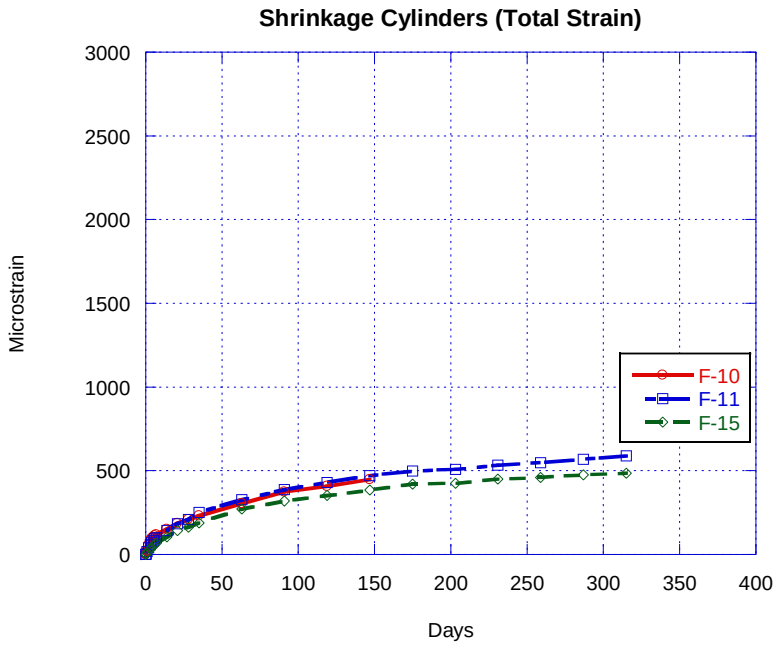

Figure 4-9 is a graphical display of how much total, creep, and free shrinkage strain induced, on average, for all cylinders for control mix.

Figure 4-9: Total, Free Shrinkage, and Creep Strain (Control)

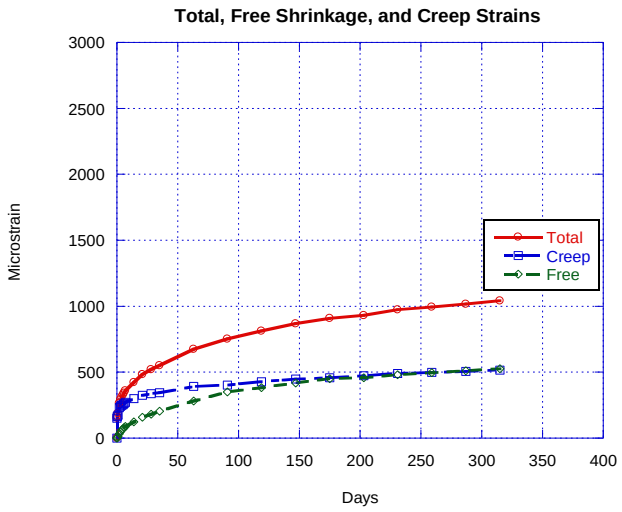

Based on **Figure 7-9**, the concrete specimens of the control mix have as much creep strain induced as free shrinkage strain by the end of the time period, which is 343 days. Total strain by the end of the process is 1042 με, free shrinkage strain is 526 με, and creep strain is 516 με.

Figure 7-10 provides graphical data of the loading variation from the load cell maintained.

Figure 7-10: Loading of Creep Cylinders (Control)

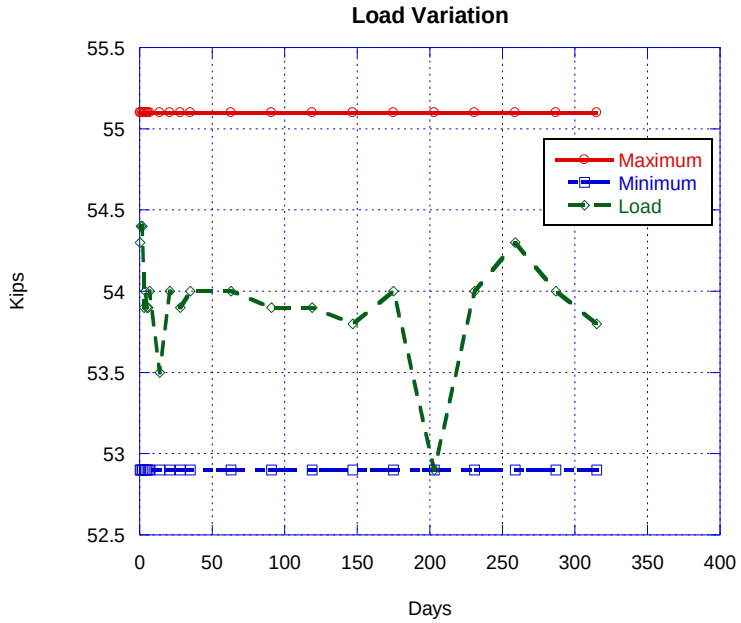

The load is maintained within the 2% range as required for creep loading and countering creep relaxation. Only once does the load nearly fall below the minimum range on day 147.

4.6.3 Polypropylene 1.5'' Mix

Figure 4-11 to 4-14 present VWSG data from the concrete specimens being tested for creep. Sensors 1 to 9 record for concrete specimens that are under load and contain creep shrinkage, while sensors 10-15 record only free shrinkage data.

Figure 4-11: Top Creep Cylinder, Sensor 1 – 3 (PPE1.5'')

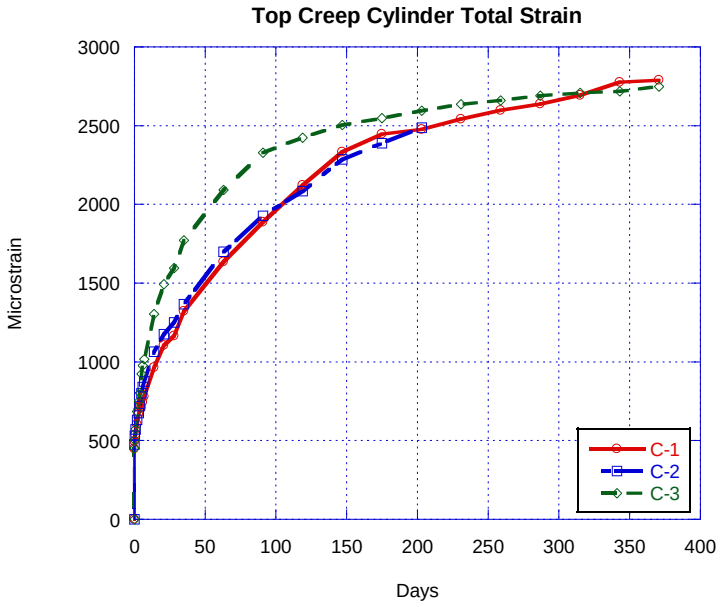

Figure 4-12: Middle Creep Cylinder, Sensors 4 – 6 (PPE1.5'')

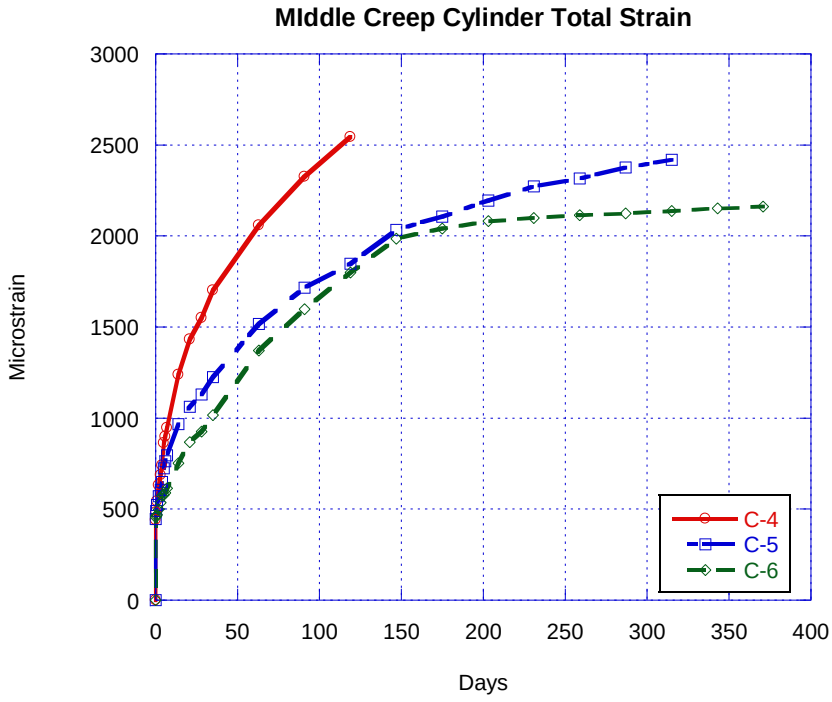

Figure 4-13: Bottom Creep Cylinder, Sensors 7 – 9 (PPE1.5'')

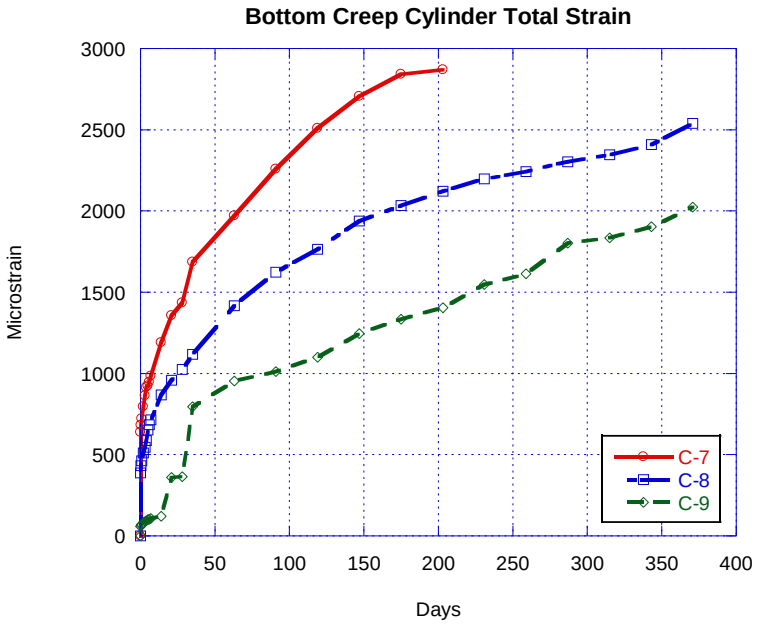

Figure 4-14: Free Shrinkage Cylinders, Sensors 10 – 15 (PPE1.5'')

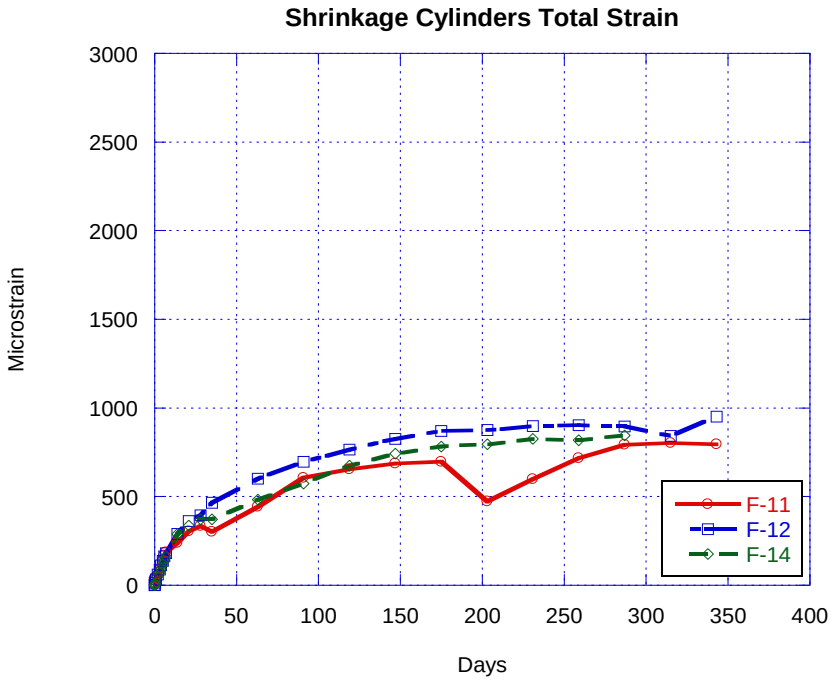

Figure 4-15 is a graphical display of how much total, creep, and free shrinkage strain is induced, on average, for all cylinders.

Figure 4-15: Total, Free Shrinkage, and Creep Strain (PPE1.5'')

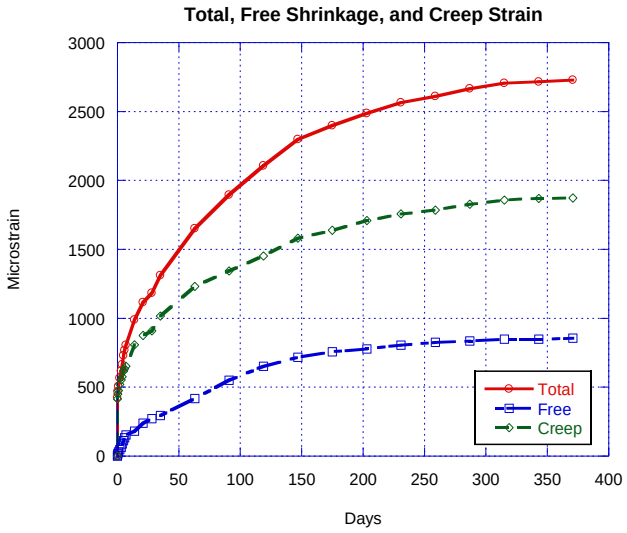

According to **Figure 4-15**, there is more than twice the amount of creep strain induced compared to free shrinkage strain. Over the span of 371 days, total strain is 2729 με, free shrinkage strain is 857 με, and creep strain is 1872 με.

Figure 4-16 presents the loading variation of the creep specimens over the period of the test.

Figure 4-16: Loading Variation (PPE1.5'')

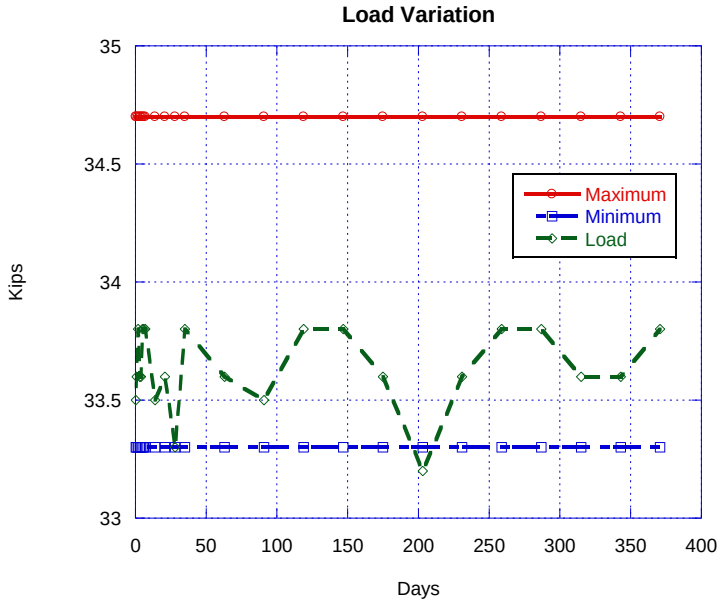

4.6.4 Polypropylene 2'' Mix

Figure 4-17 to 4-20 present VWSG data from the concrete specimens being tested for creep. Sensors 1 to 9 record for concrete specimens that are under load and contain creep shrinkage, while sensors 10-15 record only free shrinkage data.

Figure 4-17: Top Creep Cylinder, Sensors 1 – 3 (PPE2'')

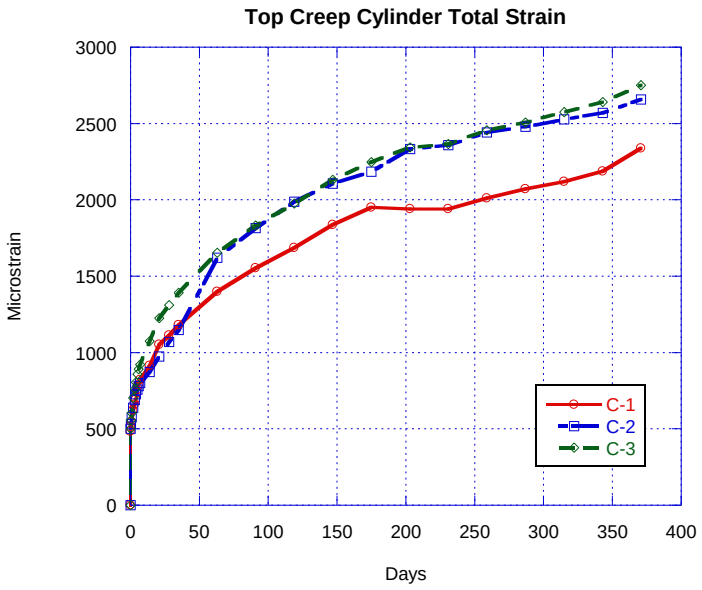

Figure 4-18: Middle Creep Cylinder, Sensors 4 – 6 (PPE2'')

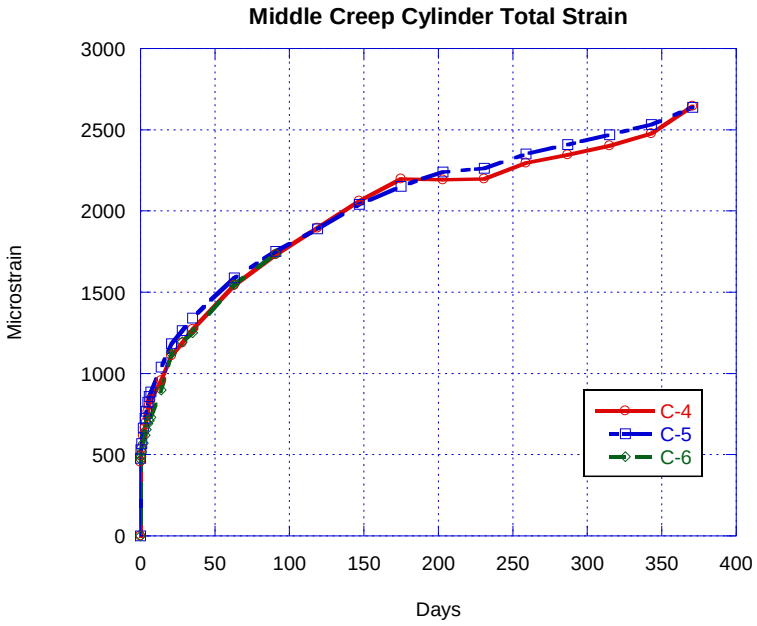

Figure 4-19: Bottom Creep Cylinder, Sensors 7 – 9 (PPE2.0'')

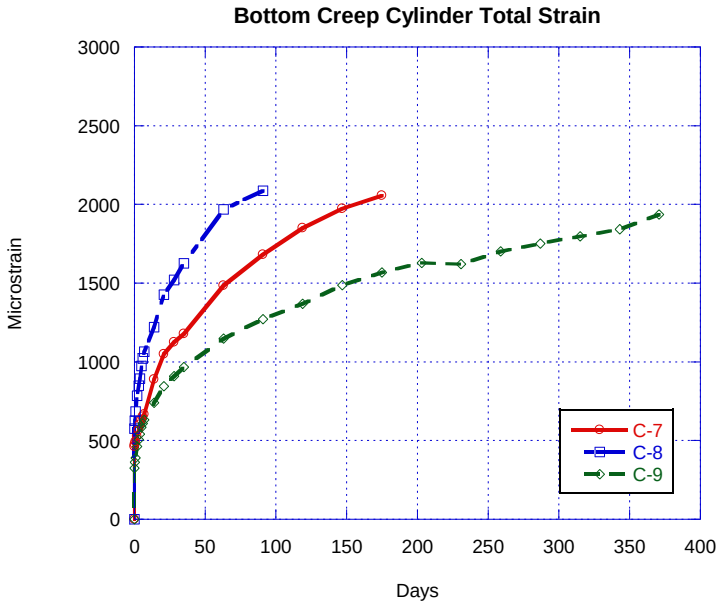

Figure 4-20: Free Shrinkage Cylinders, Sensors 10 – 15 (PPE2.0'')

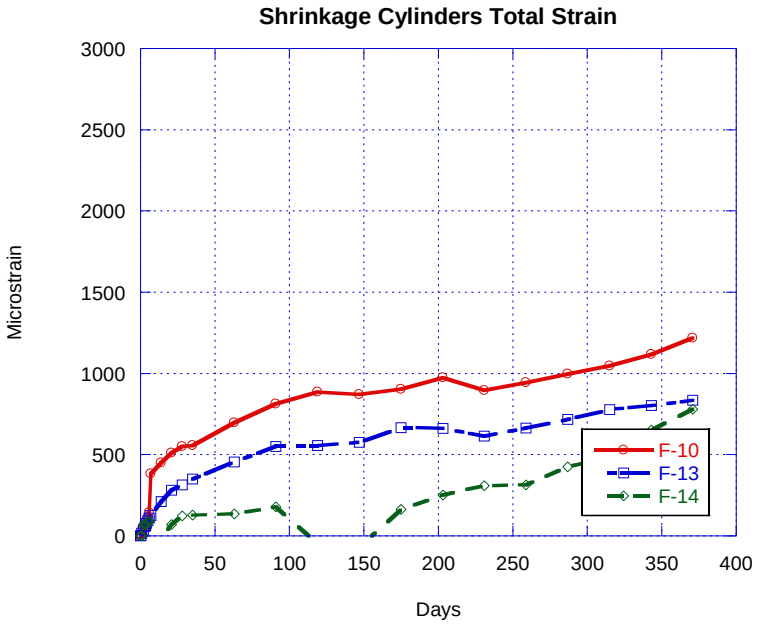

Figure 4-21 is a graphical display of how much total, creep, and free shrinkage strain is induced, on average, for all cylinders.

Figure 4-21: Total, Free Shrinkage, and Creep Strain (PPE2'')

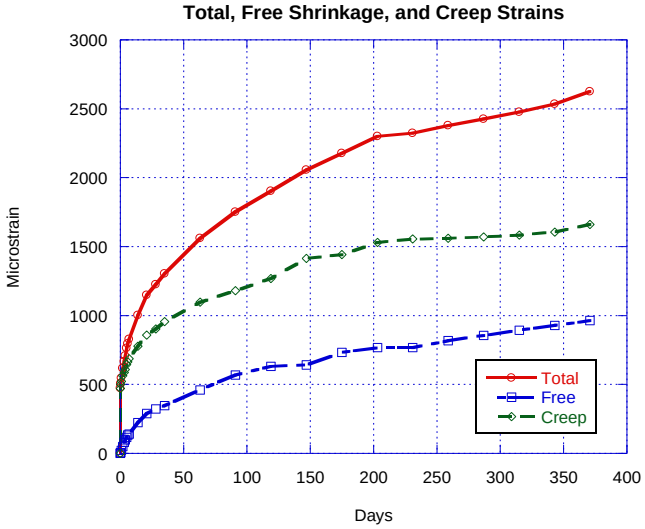

Based on **Figure 4-21**, there is almost twice as much creep strain than free shrinkage strain. Over the course of 371 days, total strain is 2625 με, free shrinkage strain is 964 με, and creep strain is 1661 με.

Figure 4-22 provides graphical data of the loading variation from the load cell maintained.

Figure 4-22: Loading Variation (PPE2'')

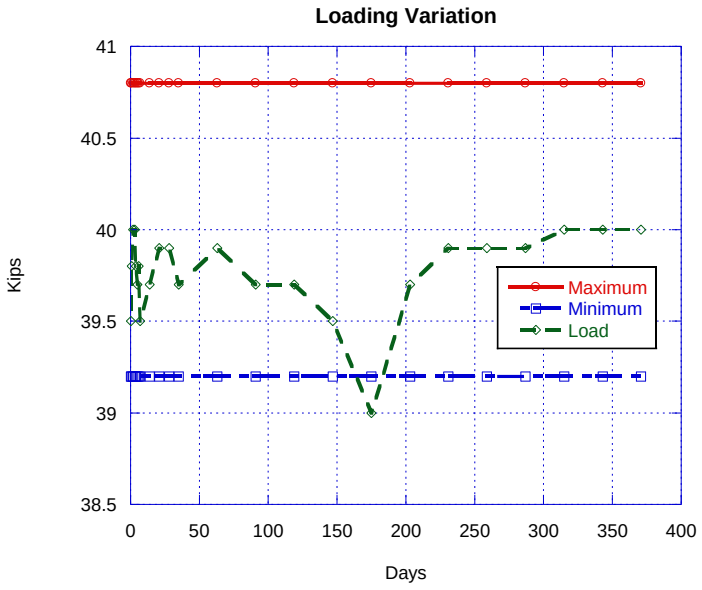

Loading is within 2% range except for on day 119 in which load decreased below the minimum.

4.6.5 Steel 1.5'' Mix

Figure 4-23 to 4-26 present VWSG data from the concrete specimens being tested for creep. Sensors 1 to 9 record for concrete specimens that are under load and contain creep shrinkage, while sensors 10-15 record only free shrinkage data.

Figure 4-23: Top Creep Cylinder, Sensors 1 – 3 (ST1.5'')

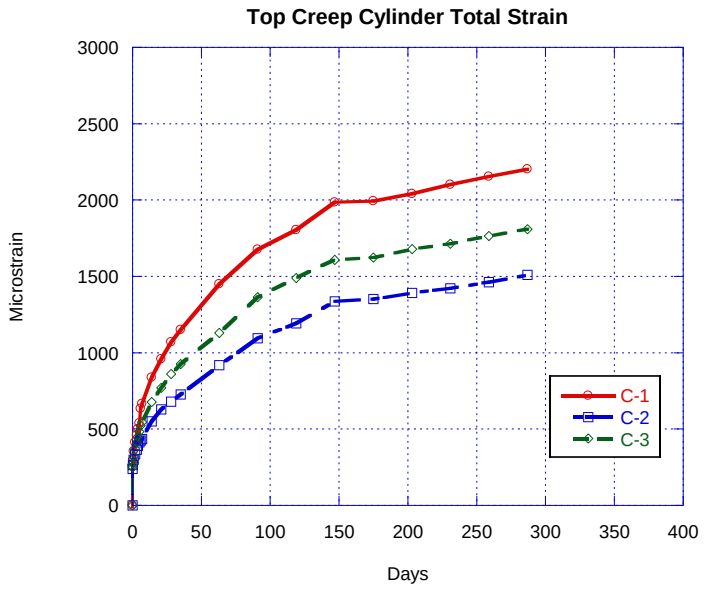

Figure 4-24: Middle Creep Cylinder, Sensors 4 – 6 (ST1.5'')

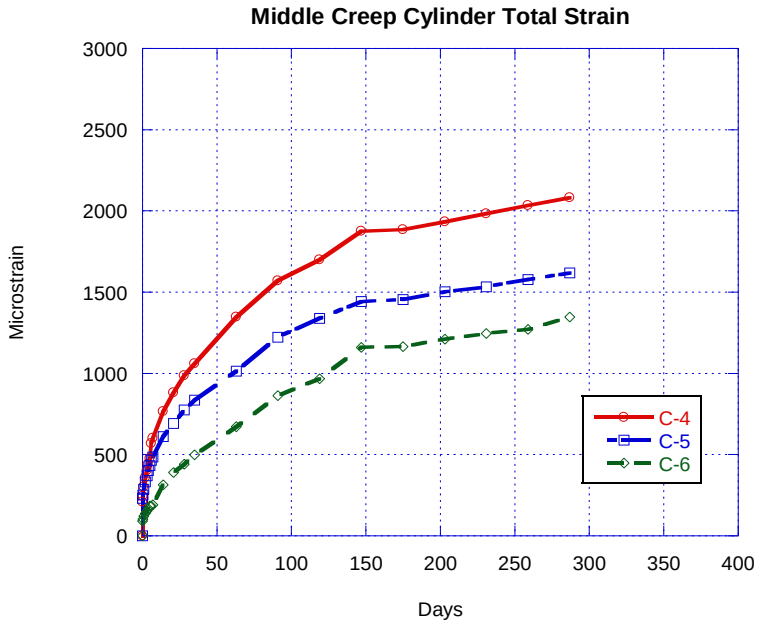

Figure 4-25: Bottom Creep Cylinder, Sensors 7 – 9 (ST1.5'')

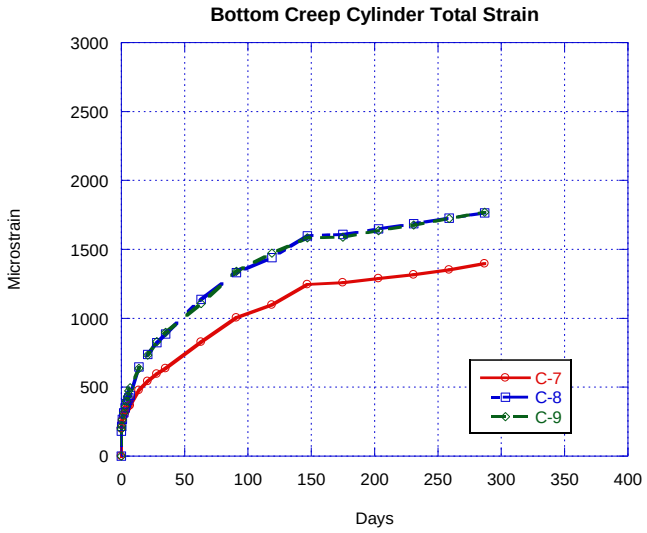

Figure 4-26: Free Shrinkage Cylinders, Sensors 10 – 15 (ST1.5'')

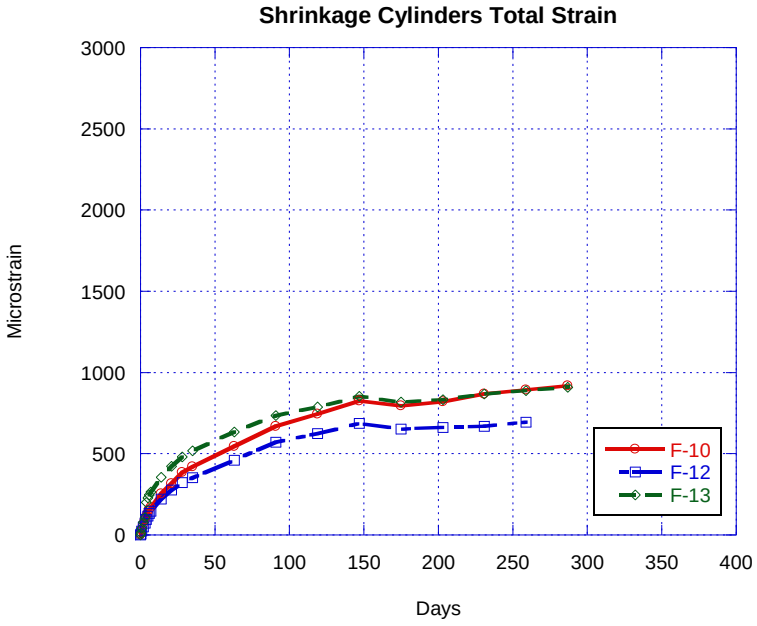

Figure 4-27 is a graphical display of how much total, creep, and free shrinkage strain is induced, on average, for all cylinders.

Figure 4-27: Total, Free Shrinkage, and Creep Strain (ST1.5'')

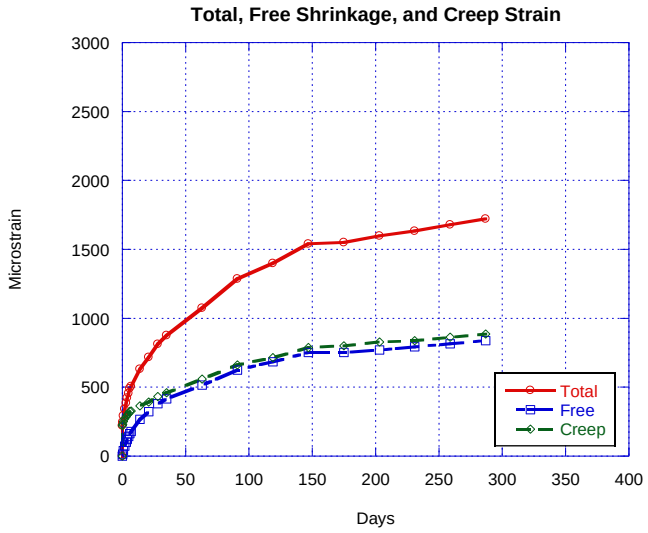

According to **Figure 4-27**, there is as much creep strain as free shrinkage strain induced. Over the course of 287 days, total strain is 1723 με, free shrinkage strain is 839 με, and creep strain is 885 με.

Figure 4-28 presents the load maintained for the steel 1.5'' mix creep specimens over the time of testing.

Figure 4-28: Loading Variation (ST1.5'')

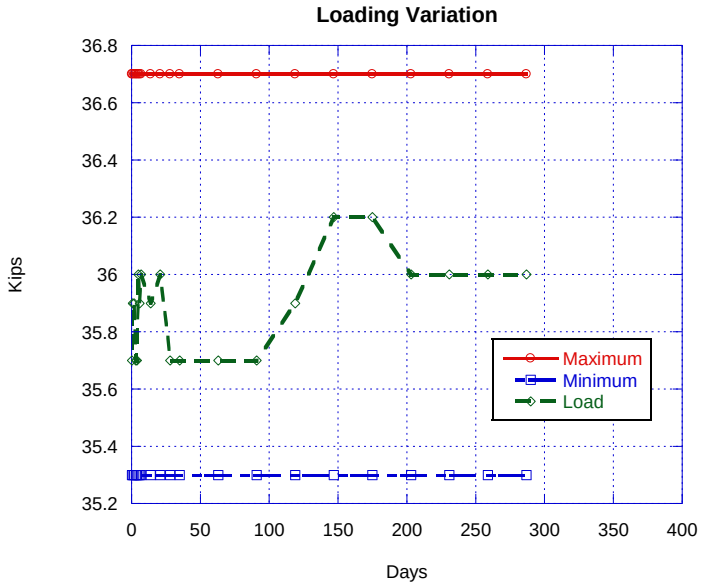

Load is maintained within the 2% range at all times and at no point does it exceed the maximum or minimum boundaries.

4.6.6 Hybrid 1 Mix

Figure 4-29 to 4-32 present VWSG data from the concrete specimens being tested for creep. Sensors 1 to 9 record for concrete specimens that are under load and contain creep shrinkage, while sensors 10-15 record only free shrinkage data.

Figure 4-29: Top Creep Cylinder, Sensors 1 – 3 (HYB-1)

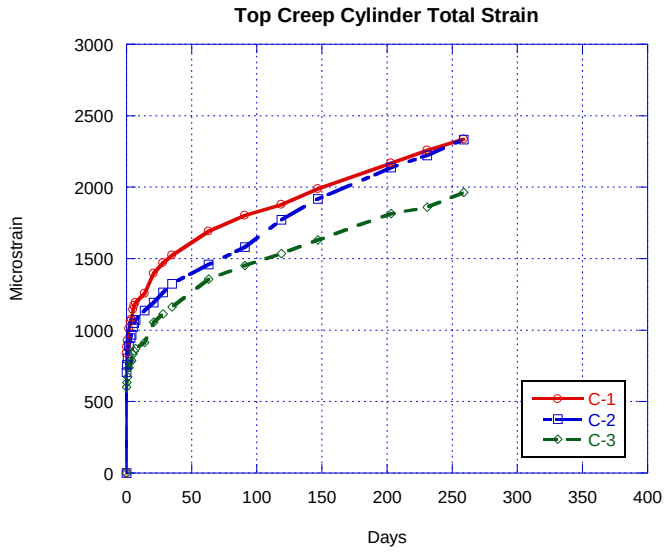

Figure 4-30: Middle Creep Cylinder, Sensors 4 – 6 (HYB-1)

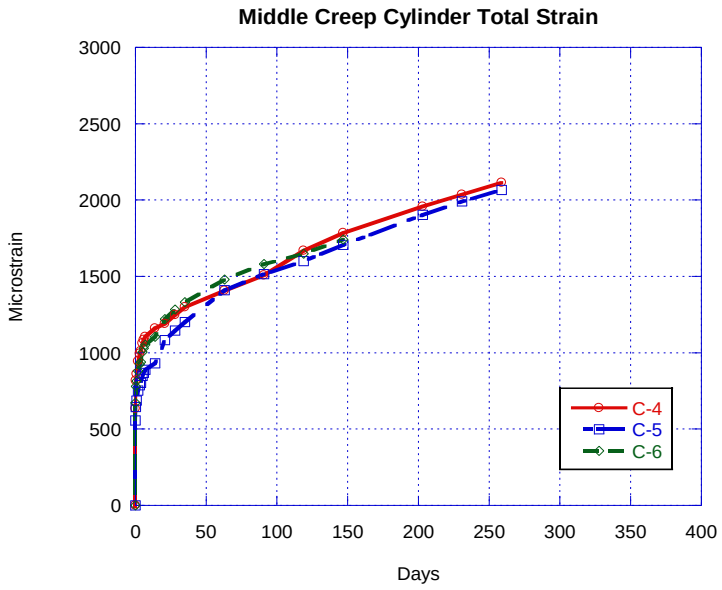

Figure 4-31: Bottom Creep Cylinder, Sensors 7 – 9 (HYB-1)

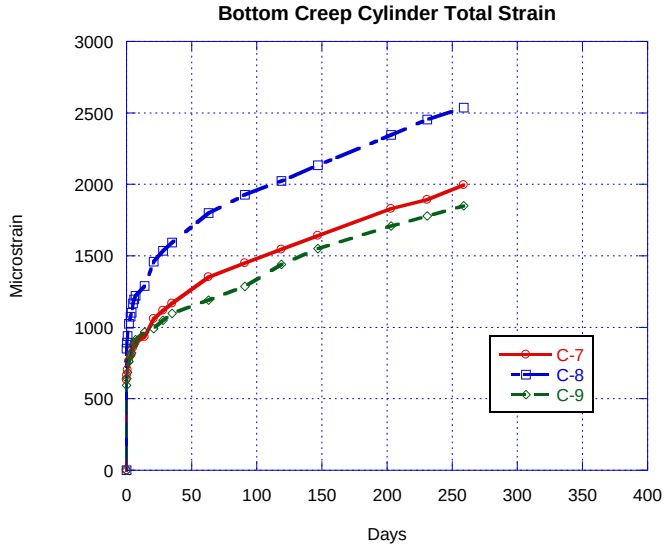

Figure 4-32: Free Shrinkage Cylinders, Sensors 10 – 15 (HYB-1)

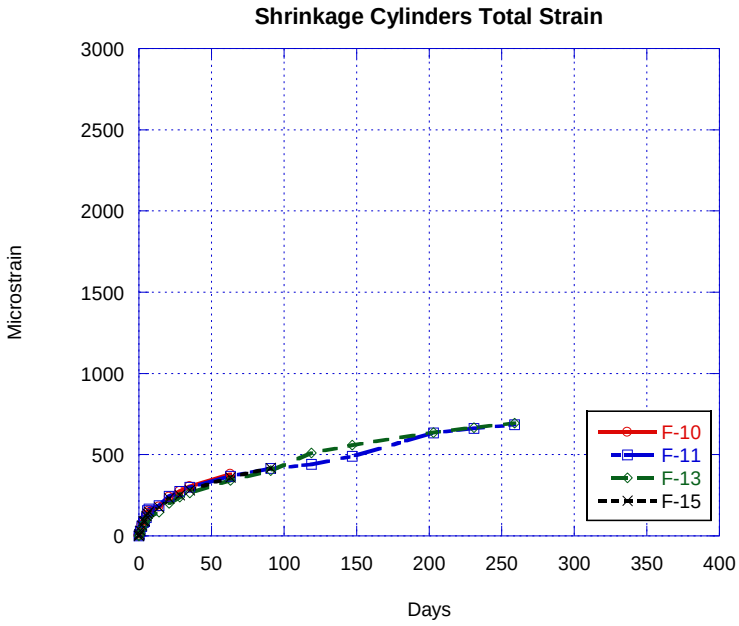

Figure 4-33 is a graphical display of how much total, creep, and free shrinkage strain is induced, on average, for all cylinders.

Figure 4-33: Total, Free Shrinkage, and Creep Strain (HYB-1)

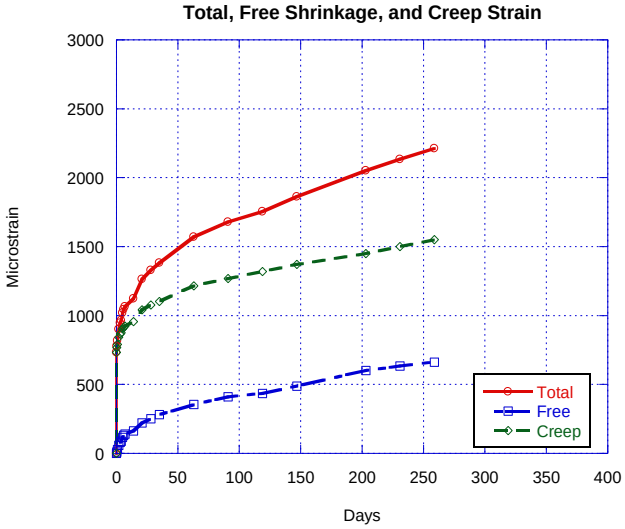

After 270 days of loading, the mix had creep strain of 1550 με, free shrinkage strain of 663 με, and a total strain value of 2213 με. There was about 25% more creep strain induced in the mix than free shrinkage.

Figure 4-34 provides graphical data of the loading variation from the load cell maintained.

Figure 4-34: Loading Variation (HYB-1)

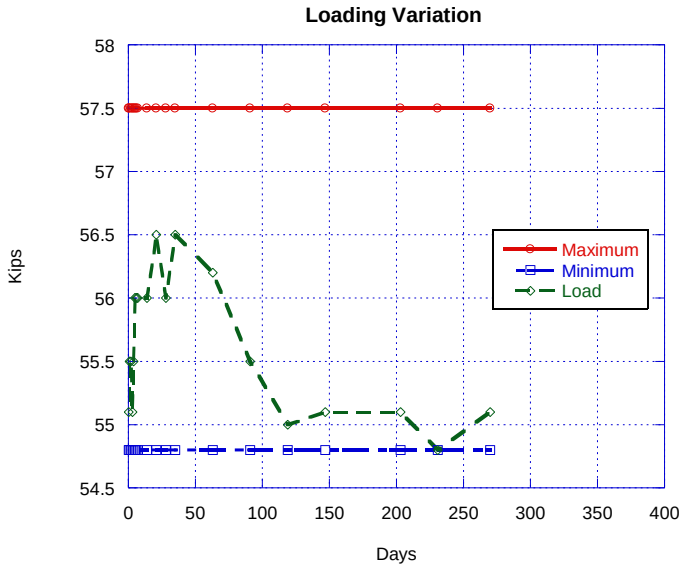

4.6.7 Hybrid 2 Mix

Figure 4-35 to 4-38 present VWSG data from the concrete specimens being tested for creep. Sensors 1 to 9 record for concrete specimens that are under load and contain creep shrinkage, while sensors 10-15 record only free shrinkage data.

Figure 4-35: Top Creep Cylinder, Sensors 1 – 3 (HYB-2)

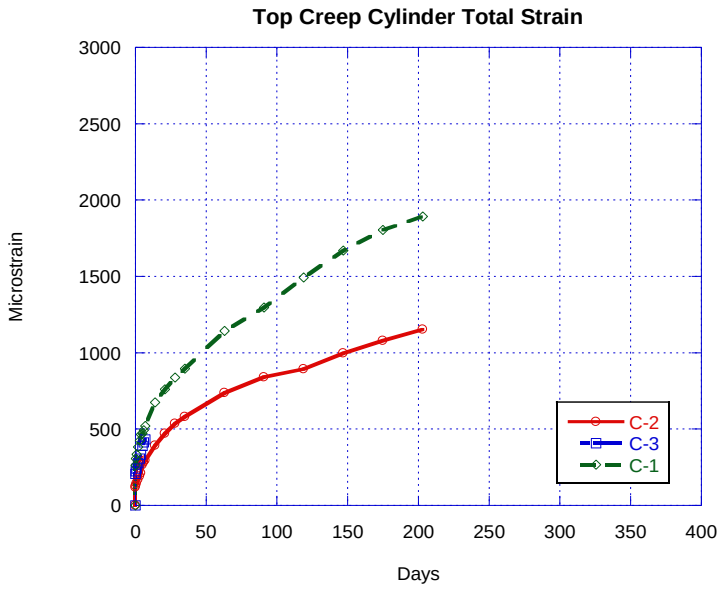

Figure 4-36: Middle Creep Cylinder, Sensors 4 – 6 (HYB-2)

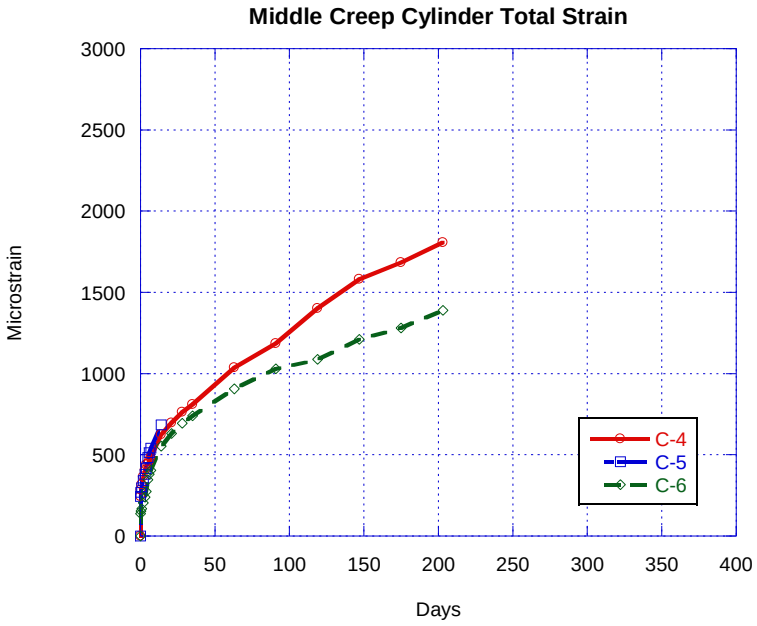

Figure 4-37: Bottom Creep Cylinder, Sensors 7 – 9 (HYB-2)

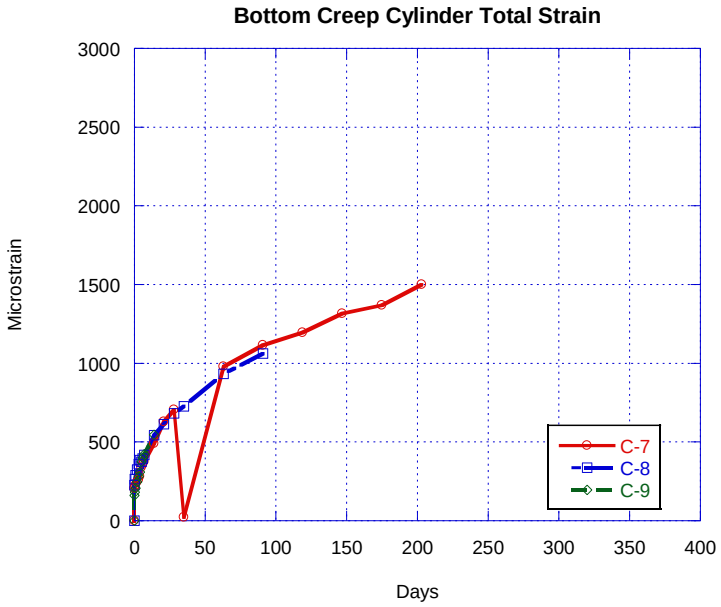

Figure 4-38: Free Shrinkage Cylinders, Sensors 10 – 15 (HYB-2)

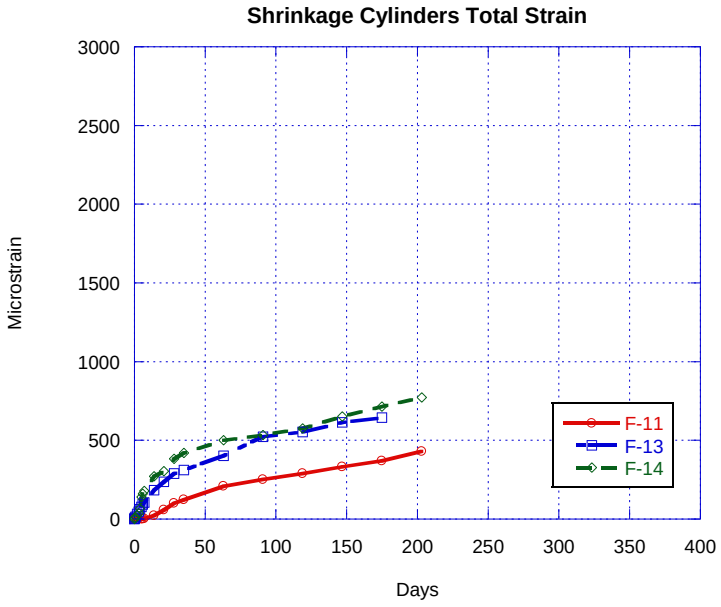

Figure 4-39 is a graphical display of how much total, creep, and free shrinkage strain is induced, on average, for all cylinders.

Figure 4-39: Total, Free Shrinkage, and Creep Strain (HYB-2)

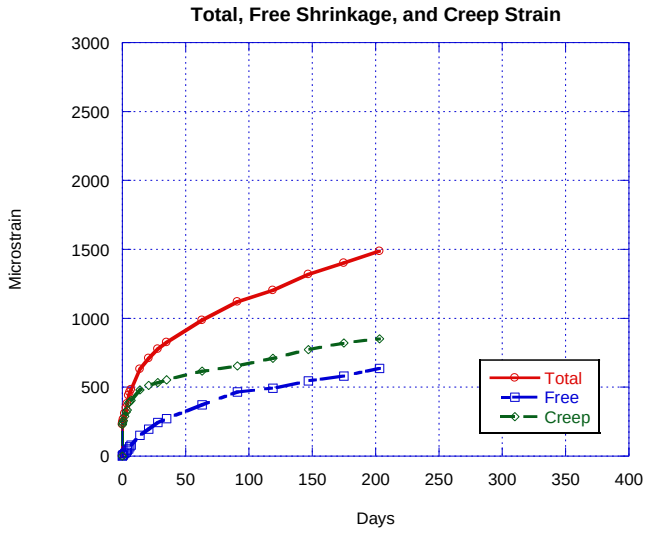

After 203 days of loading, the mix had creep strain of 852 με, free shrinkage strain of 637 με, and a total strain value of 1489 με. There was about 25% more creep strain induced in the mix than free shrinkage.

Figure 4-40 provides graphical data of the loading variation from the load cell maintained.

Figure 4-40: Loading Variation (HYB-2)

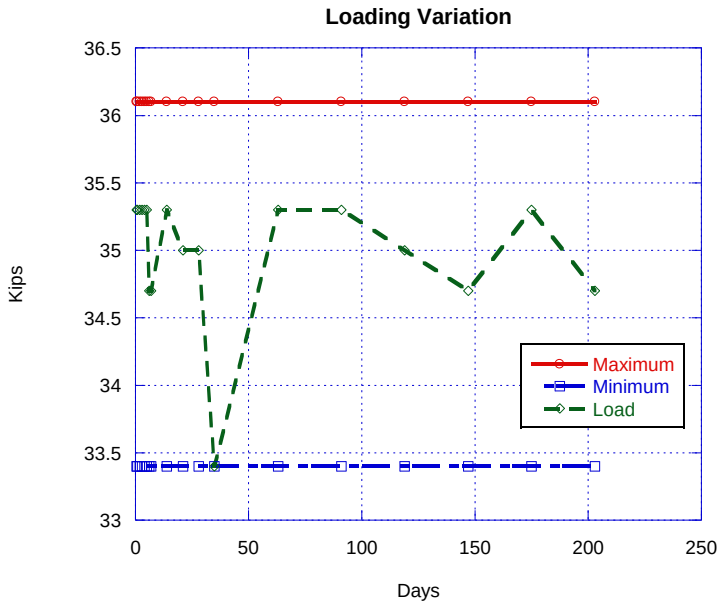

Loading has been maintained within the 2% range except during day 35 where it almost went below the minimum load range.

4.7 Fiber Influence

Table 4-7 displays final total strain values for all mixes as well as the percentages of free and creep that made up the total strains over their respective period of monitoring.

Table 4-7: Final Total Strain Values and Proportions

	Control	PPE1.5''	PPE2''	ST1.5''	HYB-1	HYB-2
Total (με)	1042	2729	2625	1723	1489	2213
Free Shrinkage (%)	50.5	31.4	36.7	48.7	42.8	30
Creep (%)	49.5	68.6	63.3	51.3	57.2	70
Load (psi)	1908	1202	1415	1238	1980	1238

According to the table, the presence of polypropylene fibers, macro and/or micro size, consistently causes an increase in creep strain. A dosage of 5 lb/yd^3 of either 1.5'' or 2'' macro polypropylene fibers cause an increase of creep strain by at least 13% but also reduce free shrinkage by at least 13%. Additionally, a combination of micro and macro polypropylene fibers increases creep strain by almost 20% but also reduces free shrinkage by 20%. This is accurate with the purpose of polypropylene fibers reducing free shrinkage of SCC, and it also indicates that the presence of polypropylene fibers can also cause more creep strain than conventional SCC mixes without fibers. Regarding the steel fibers, the results from ST1.5'' and HYB-1 indicate that although the fibers do not decrease free shrinkage as much as polypropylene fibers, they do not cause as much creep strain increase/

Inclusion of both types of fibers (HYB-1) at half the dosages still causes a reasonable increase of creep strain by about 7%, yet free shrinkage is also reduced by 7%. Therefore, the

influence from macro polypropylene fibers are shown to be more impactful than the influence from steel fibers. Furthermore, the presence of micro polypropylene fibers provides as much influence to creep and free shrinkage as macro polypropylene fibers. Reducing the macro polypropylene fiber dosage by half and replacing with micro polypropylene fiber dosage still causes almost the same amount of free shrinkage decrease and creep increase.

Figure 4-41 displays the specific creep comparison between all mixes over the course of their respective time of loading.

Figure 4-41: Specific Creep of All Mixes

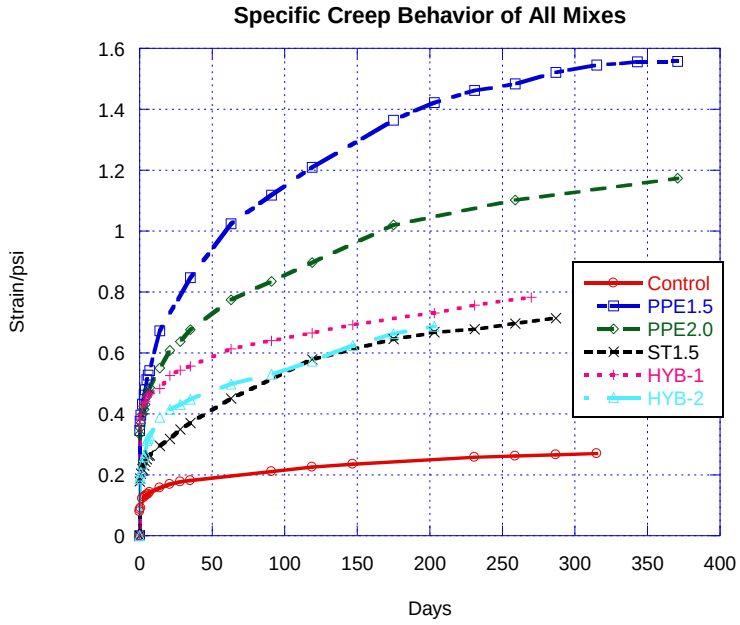

Based on results of 315 days, the presence of 1.5'' and 2'' macro polypropylene fibers increase specific creep about 5.7 times and 4.2 times, respectively; and based on 287 day results, the presence of 1.5'' steel fibers increase specific creep by about 2.8 times. Based on results on 231 days, a combination of steel and macro polypropylene fibers, both 1.5'' in length, increases

specific creep about 3 times. Based on results of 203 days, the combination of macro and micro polypropylene fibers increases specific creep about 2.7 times.

The presence of either 1.5'' or 2'' macro polypropylene fibers alone increase specific creep the most, with the presence of steel fibers alone being the least. The inclusion micro polypropylene fibers results in a severe reduction in macro polypropylene fibers' influence in specific creep. Furthermore, the presence of steel fibers in any mix is able to either reduce specific creep the most or reduce the influence of macro polypropylene fibers as much as the micro polypropylene fibers.

CHAPTER V

5. CREEP AND SHRINKAGE MODELING

5.1 Introduction

The following chapter provides a comparison between the experimental data including creep and shrinkage results to predicted results based off of 4 creep models. Models include ACI209, B3, CEB, and GL2000 for prediction of creep and shrinkage. Because of the unknown influence of the fibers, creep and shrinkage equations are modified and presented with proper regression analysis to accommodate.

5.2 Comparison of Experimental Shrinkage and Predicted Shrinkage

Figures 5-1 to 5-6 present the comparison between experimental shrinkage and predicted shrinkage for all six mixes and for all four creep models discussed for this research.

Figure 5-1: Control Mix, Experimental vs. Predicted Shrinkage

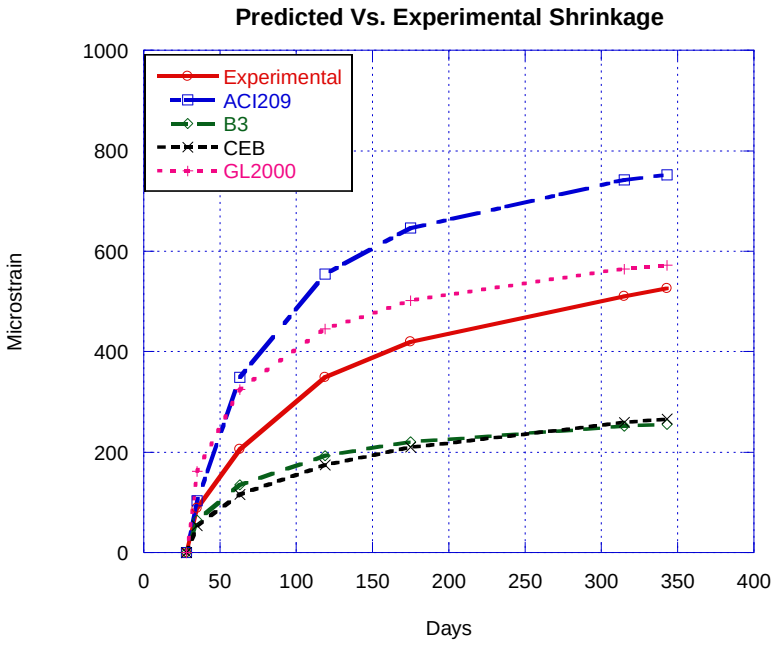

The ACI209 and GL2000 models overestimate experimental free shrinkage strain; and the CEB and B3 models underestimate it.

Figure 5-2: Polypropylene 1.5'' Mix, Experimental vs. Predicted Shrinkage

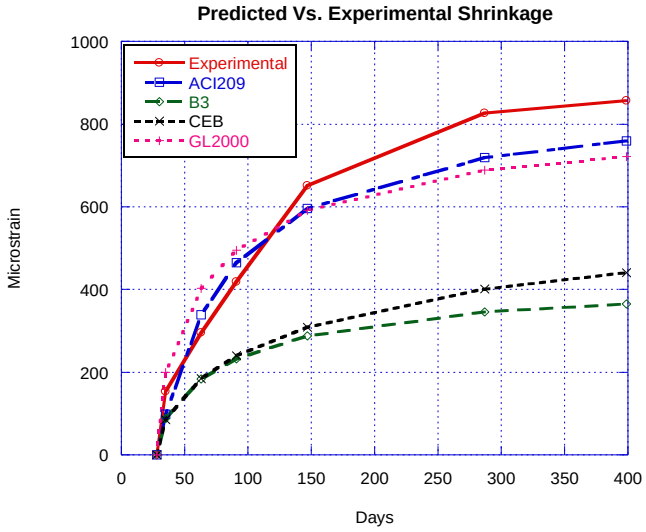

All models in this research study underestimate experimental free shrinkage strain of this mix.

Figure 5-3: Polypropylene 2'' Mix, Experimental vs. Predicted Shrinkage

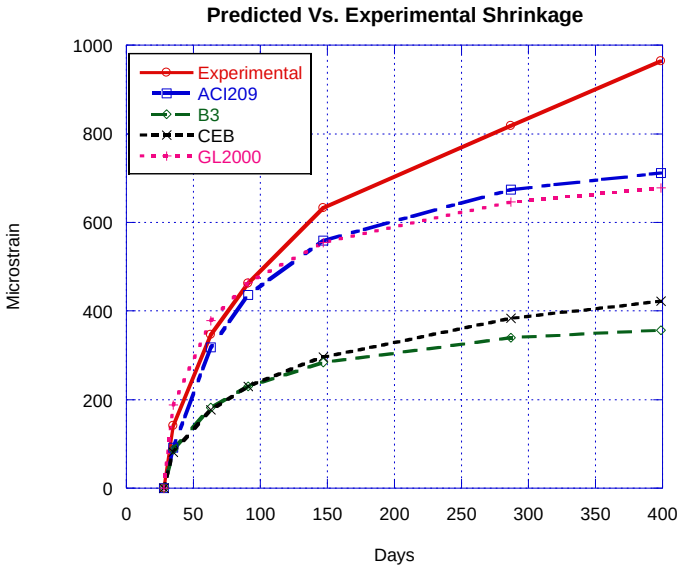

All models in this research study underestimate the experimental free shrinkage strain of this mix.

Figure 5-4: Steel 1.5'' Mix, Experimental vs. Predicted Shrinkage

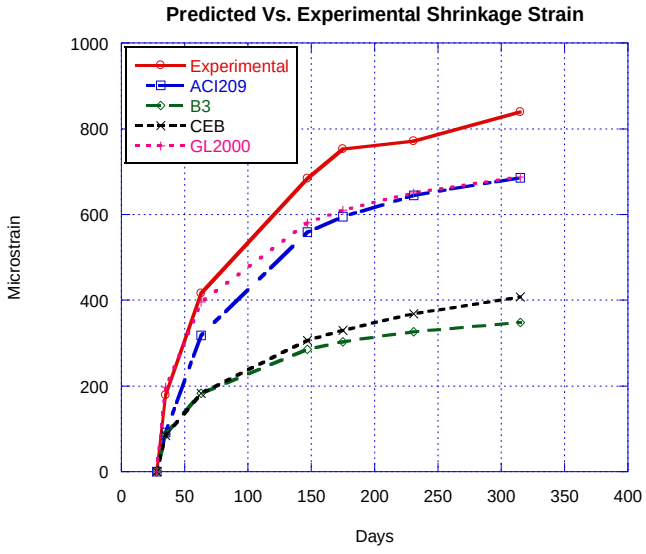

All models underestimate the experimental free shrinkage strain of this mix.

Figure 5-5: Hybrid 1 Mix, Experimental vs. Predicted Shrinkage

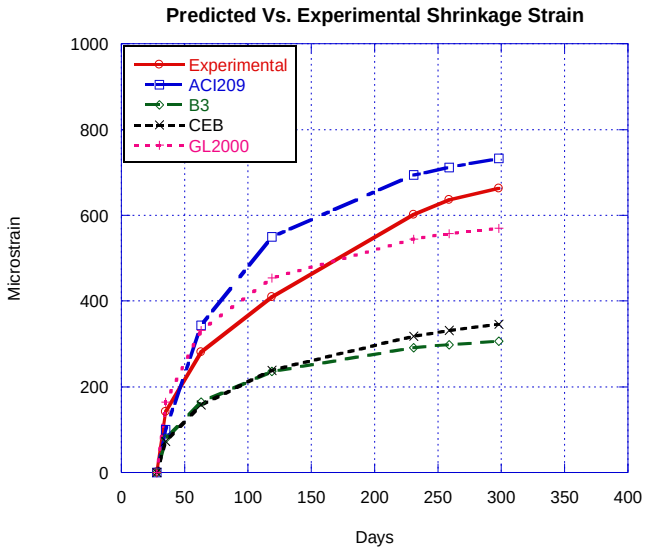

Only ACI209 overestimates shrinkage of this mix, while the rest of the models underestimate shrinkage.

Figure 5-6: Hybrid 2 Mix, Experimental vs. Predicted Shrinkage

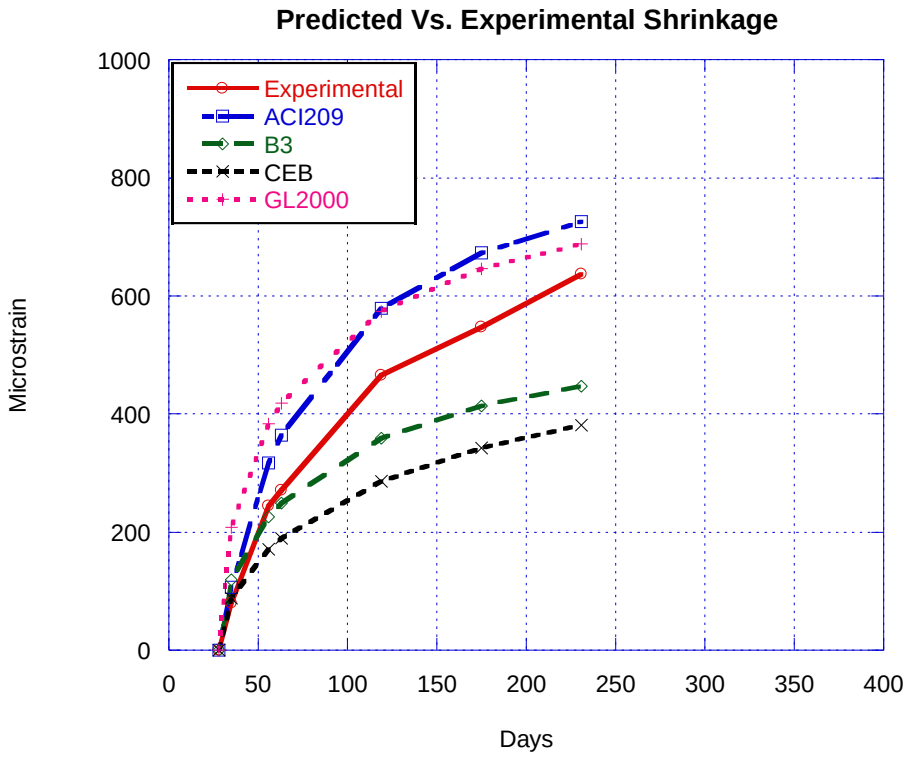

Both ACI209 models and the GL2000 model overestimate free shrinkage of the mix, while CEB and B3 underestimate it.

5.3 Comparison of Experimental Creep and Predicted Creep

Figures 5-7 to 5-12 present the comparison between experimental shrinkage and predicted shrinkage for all six mixes and for all four creep models discussed for this research.

Figure 5-7: Control Mix, Experimental Vs. Predicted Creep

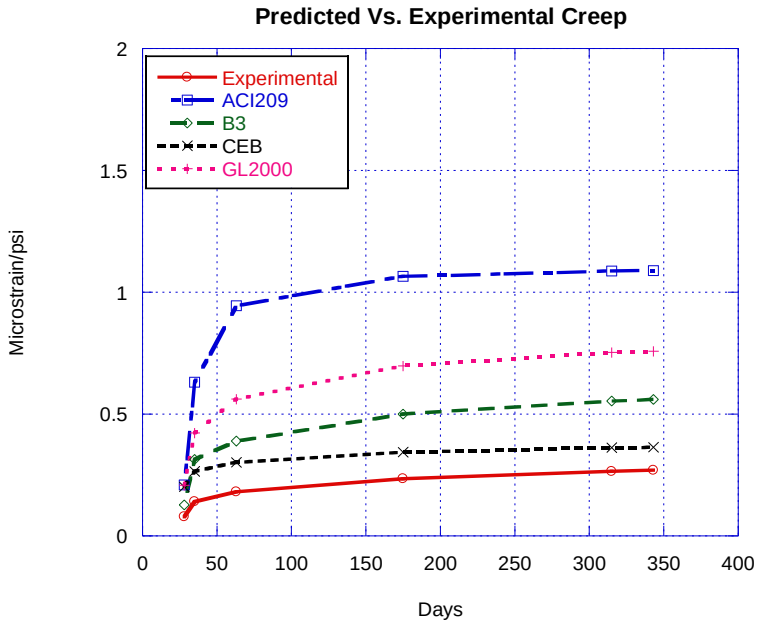

All models overestimate the experimental creep strain for this mix.

Figure 5-8: Polypropylene 1.5'' Mix, Experimental vs. Predicted Creep

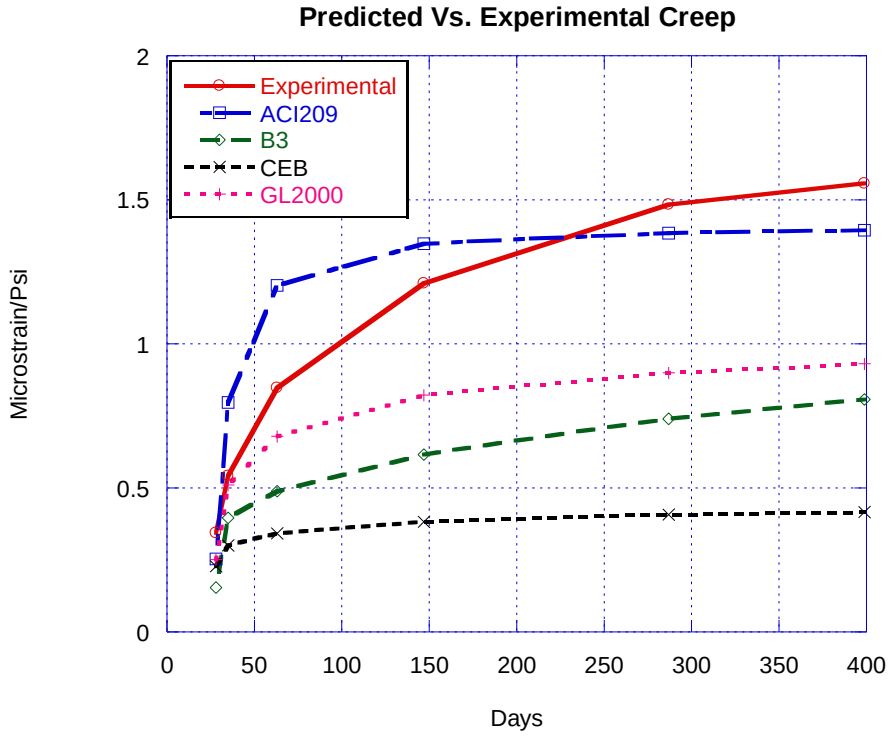

All models underestimate experimental creep strain, except for the ACI209 model which overestimated experimental creep strain before 287 days of age.

Figure 5-9: Polypropylene 2'' Mix, Experimental vs. Predicted Creep

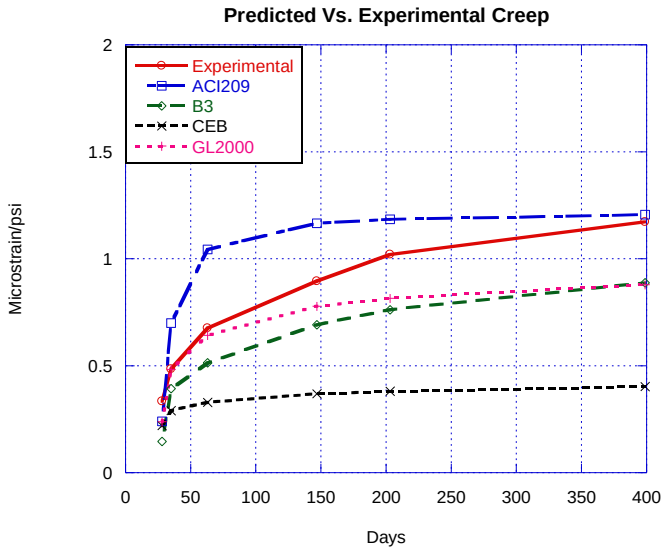

All models underestimate experimental creep strain, except for ACI209 model which overestimates the experimental creep strain.

Figure 5-10: Steel 1.5'' Mix, Experimental vs. Predicted Creep

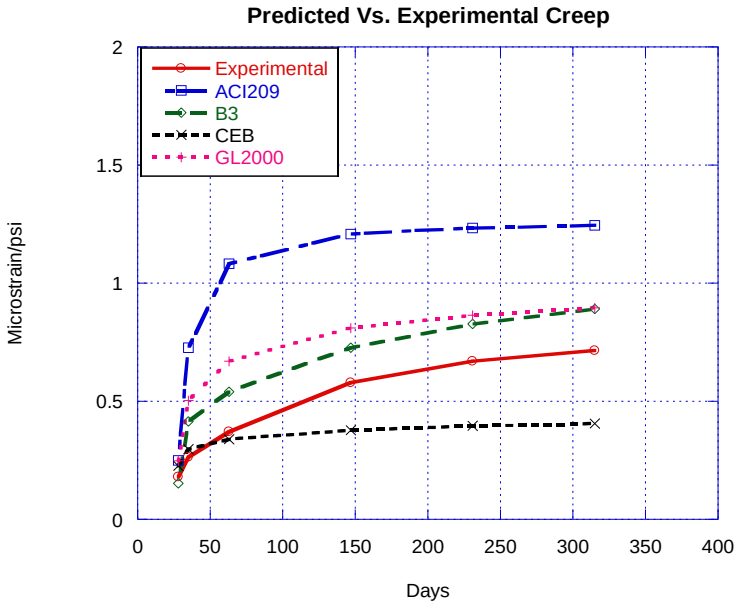

Only the CEB model underestimates the experimental creep strain; all other models overestimate the experimental strain.

Figure 5-11: Hybrid 1 Mix, Experimental vs. Predicted Creep

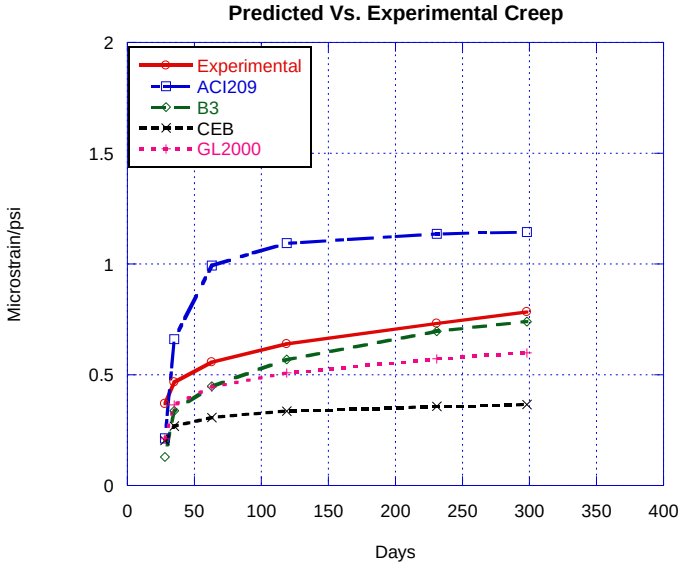

Only ACI209 overestimates the creep behavior of this mix; the other three creep models underestimate creep behavior.

Figure 5-12: Hybrid 2 Mix, Experimental vs. Predicted Creep

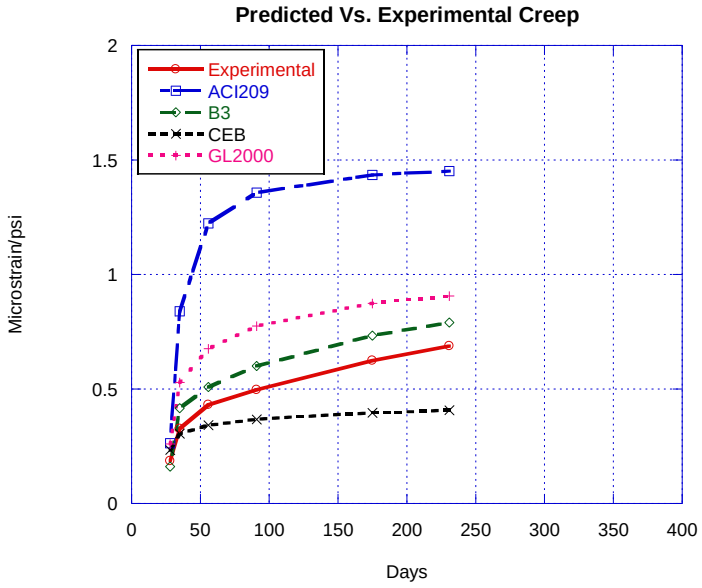

All models overestimate the experimental creep strain except for the CEB model.

In order to determine the precision between the experimental and predicted data based on the graphical behavior shown, linear regression analysis is performed for all mixes and all models. **Table 5-1** provides the coefficient of correlation factors for creep and shrinkage for all mixes.

Table 5-1: Coefficient of Correlation Factor for Creep and Free Shrinkage

	Control		Polypropylene 1.5''		Polypropylene 2''		Steel 1.5''		Hybrid 1		Hybrid 2	
Models	**Creep R^2**	**Shrinkage R^2**	**Creep R^2**	**Shrinkage R^2**	**Creep R^2**	**Shrinkage R^2**	**Creep R^2**	**Shrinkage R^2**	**Creep R^2**	**Shrinkage R^2**	**Creep R^2**	**Shrinkage R^2**
ACI 209	0.912	(f = 35) 0.990 (f = 108) 0.606	0.817	(f = 35) 0.973 (f = 108) 0.548	0.817	(f = 35) 0.975 (f = 108) 0.952	0.790	(f = 35) 0.995 (f = 108) 0.514	0.841	(f = 35) 0.979 (f = 108) 0.536	0.869	(f = 35) 0.993 (f = 108) 0.527
B3	0.990	0.982	0.956	0.966	0.977	0.966	0.957	0.997	0.988	0.977	0.983	0.976
CEB	0.991	0.997	0.946	0.986	0.943	0.994	0.920	0.993	0.952	0.995	0.966	0.990
GL2000	0.987	0.969	0.936	0.942	0.934	0.946	0.910	0.992	0.965	0.965	0.959	0.954

For modeling creep of fiber reinforced self-compacting concrete, the Bazant Baweja B3 model is considered the most accurate with all coefficient of correlation factors being above 95% while ACI209 is the least accurate model with factors being as low as 79%. With regard to shrinkage, CEB is considered the most accurate with factors being as high as almost 99% consistently for all mixes; while, GL2000 is the least accurate model with factors being as low as 94% for all mixes.

5.3.1 Adjustment Factors for Creep Prediction for Bazant-Baweja B3 Model

The following correction factors have been created to increase accuracy of the B3 Model to creep data of FR-SCC mixes. It is noted that these factors are multiplied to the f_{cm28} values of the B3 Model and are determined based on the type of fiber included.

$$\boldsymbol{0.6}\ x\ f_{cm28}\ \textit{(Polypropylene Fibers)}$$

$$\boldsymbol{1.5}\ x\ f_{cm28}\ \textit{(Steel Fibers)}$$

$$\boldsymbol{1.05}\ x\ f_{cm28}\ \textit{(Hybrid of Steel and Polypropylene Fibers)}$$

The following factors can be readily applied to their respective fiber type to ensure that the B3 model is able to have more accurate data to FR-SCC creep behavior. Due to the behavior of the experimental data and model, no appropriate correction factor has been made to the hybrid fiber combination of macro and micro polypropylene fibers. **Figure(s) 5-13 to 5-16** present the new correlation between the experimental data and B3 model data with the correction factors included.

Figure 5-13: New Correlation Between B3 Model and Experimental Data (PPE1.5'')

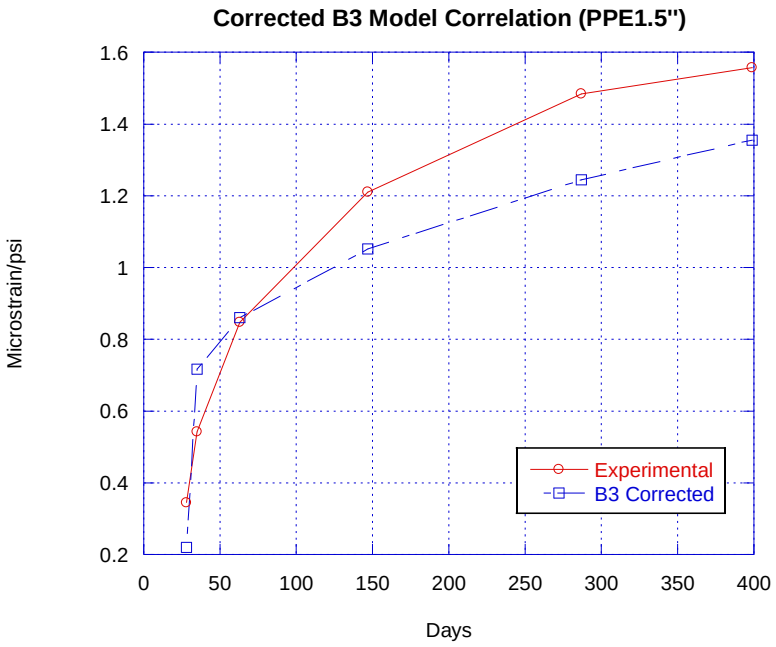

Figure 5-14: New Correlation Between B3 Model and Experimental Data (PPE2.0'')

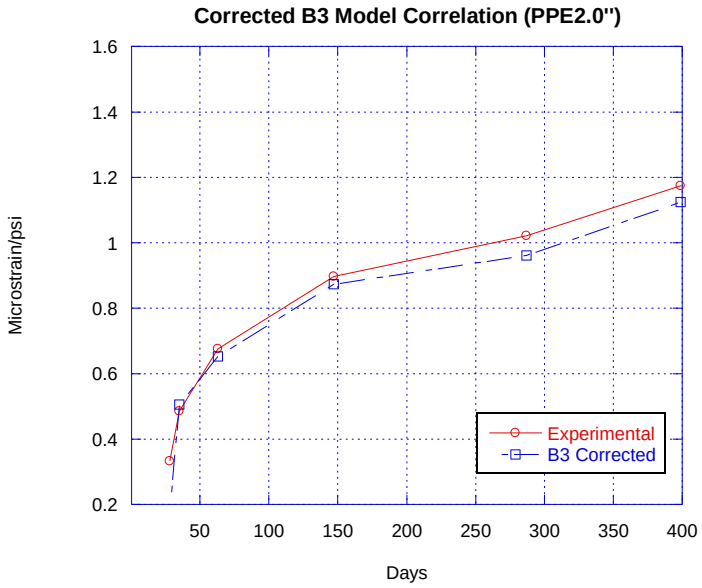

Figure 5-15: New Correlation Between B3 Model and Experimental Data (ST1.5'')

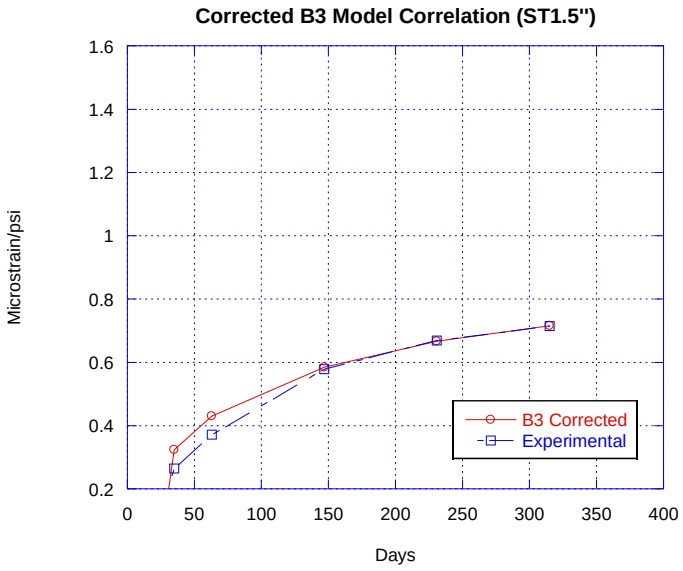

Figure 5-16: New Correlation Between B3 Model and Experimental Data (HYB-1)

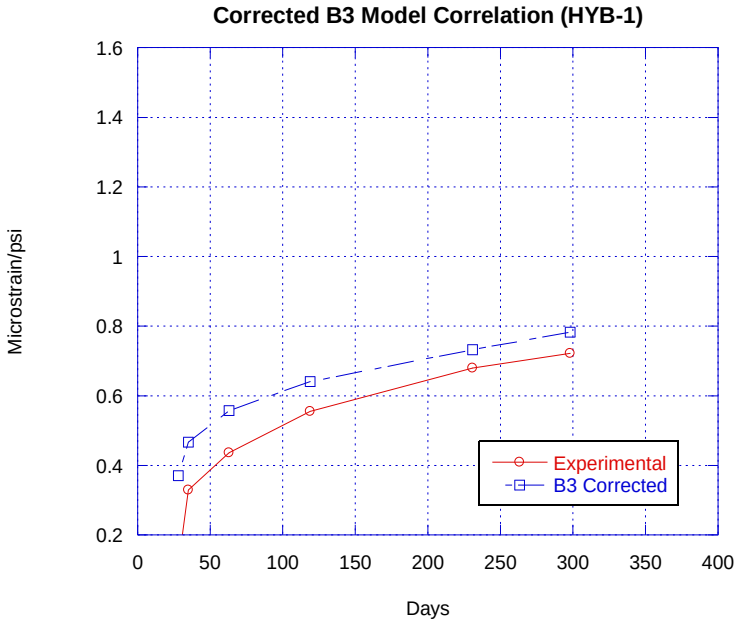

CHAPTER VI

6. SUMMARY AND CONCLUSION

6.1 Conclusion

This study was intended to investigate the effects of the polypropylene and steel fibers as well as the combination of the two types regarding creep performance. Furthermore, the creep behavior for these types of concrete mixes was evaluated using the four models: ACI209, B3, CEB, and GL2000 based on specific creep results. Based on the accuracy between the experimental and predicted results for each mix and model, one model is recommended for creep and shrinkage.

The following conclusions can be gathered from this study:

1. Regarding fresh concrete properties, the 2.0-inch macro polypropylene fibers and 0.75'' micro fibers are the strongest influences in reducing flow ability of self-consolidating concrete, especially in dense reinforcement conditions.
2. The macro polypropylene fibers, especially of length 1.5 inches, performed the best with respect to enhancing hardened concrete properties of self-consolidating concrete. The macro fibers were able to retain the most compressive strength, elasticity, and flexural strength compared to other fibers, but increased permeability of concrete the most, risking more corrosion issues. Steel fibers performed best only in reducing permeability of concrete in this study. Furthermore, the 1.5'' macro polypropylene fibers were most efficient in reducing shrinkage strain of the concrete over 28 days; micro fibers at half recommended dosage had as much influence in reducing shrinkage as 2.0'' macro polypropylene fibers with full dosage.
3. While the 1.5'' macro polypropylene fibers performed best with hardened concrete properties, they induced the most creep strain compared to the other fiber types. On

the other hand, steel fibers were the most effective in resisting creep strain and its influence on creep had more significance than that of the macro polypropylene fibers.

4. When comparing the experimental data with the discussed creep and shrinkage models through linear regression analysis, it was determined that Bazant Baweja B3 was most effective in predicting creep behavior for FR-SCC mixes while CEB was most effective in predicting shrinkage behavior.
5. Correction factors have been created and implemented to the B3 Model to accommodate for the creep behavior of FR-SCC. Although the adjustment works well for single-type fiber reinforced self-consolidating concrete mixes, the correction factors do not adjust as properly for mixes with hybrid fiber combinations.

6.2 Future Work and Recommendations

Only two hybrid-fiber mixes are studied in this research for creep behavior of self-consolidating concrete; and based on the responsiveness of the fibers to the adjusted B3 model, there is much more analysis needed for fiber combinations of polypropylene and steel fibers. Furthermore, more research is required to determine how the presence of micro polypropylene fibers can solely influence creep and shrinkage of SCC mixes since they were only present as a mixture with macro polypropylene fibers.

Moreover, more improvement is needed on the correction factors for adjusting the B3 model for FR-SCC mixes as they account for a very limited amount of fiber types and content. A primary recommendation for continuing with this research study is to include other fiber types such as nylon or glass fibers or straight or hooked steel fibers to determine how they may influence creep behavior of SCC mixes and how well the factors predicts creep. Additionally,

more fiber variations of micro polypropylene fibers should be analyzed for further understanding of the influence of these fibers on creep behavior of FR-SCC.

REFERENCES

1. Goodier C.I., "Development of self-compacting concrete" *Proceedings of the ICE- Structure and Buildings*, Vol.4, pp.405-414, 2003
2. Bazant P.Z., "Theory of Creep and Shrinkage in Concrete Structures: A Precis of Recent Developments," *Mechanics Today*, Vol. 2, Ch.1, pp.1-93, 1975
3. "Concrete in Practice: What, why, & how?", *NRMCA, 2004* https://www.nrmca.org/aboutconcrete/cips/37p.pdf
4. "Definitions of Terms Relating to Self-Consolidating Concrete (SCC)," *GCP Applied Technologies*, 2008 https://ca.gcpat.com/sites/ca.gcpat.com/files/2017-06/Technical-Bulletin-TB-1501_v2%20%282%29.pdf
5. K. H. Khayat, "Workability, Testing, and Performance of Self-Consolidating Concrete*," ACI Materials* Journal, No. 96-M43, pp.346-353, 1999
6. "Scientific Principles," *Mast*, Accessed 19 July 2018 http://matse1.matse.illinois.edu/concrete/prin.html
7. Khalell R. O., Al-Mishhadani A. S., Abdul Razak H., "The Effect of Coarse Aggregate on Fresh and Hardened Properties of Self Compacting Concrete (SCC*)," Procedia* Engineering, Vol. 14, pp.805-813, 2011
8. Boukendakji O., Kenai S., Kadri E.H., Rouis F., "Effect of slag on the rhelogy of fresh self-compacted concrete*," Construction and Building* Materials 2009
9. "Ground Granulated Blast-Furnace Slag: Its Chemistry and Use with Chemical Admixtures," *GCP Applied Technologies*, Accessed 19 July 2018 https://gcpat.com/sites/gcpat.com/files/2017-06/Technical-Bulletin-TB-0102_v2.pdf

10. Cervantes V., Roesler J., "Ground Granulated Blast Furnace Slag," *Center of Excellence For Airport Technology*, Accessed 18 July 2018 https://pdfs.semanticscholar.org/b14e/fb995bb997c1d7d7cceeebafe57ba2d299d6.pdf

11. Panarese C. William, "How to Use Air-Entrained Concrete… And Why You Should Use It," *Concrete Construction* Accessed 19 July 2018 https://www.concreteconstruction.net/how-to/materials/how-to-use-air-entrained-concrete-and-why-you-should-use-it_o

12. Titin Handojo, "Use of Water Reducers, Retarders, and Superplasticizers," Accessed 19 July 2018 http://www.engr.psu.edu/ce/courses/ce584/concrete/library/materials/Admixture/AdmixturesMain.htm

13. "Plastol 5000: High Range Water Reducing Admixture," *Euclid Chemical* Accessed 19 July 2019 https://www.euclidchemical.com/fileshare/ProductFiles/tds/plastol_5000.pdf

14. Wafa F. F., "Properties and Applications of Fiber Reinforced Concrete," *Engineering Sci.* Vol. 2, pp.49-63, 1990

15. Concrete Construction Staff, "Concrete Reinforced With Polypropylene Fibers," *Concrete Construction* Accessed 19 July 2019 http://www.concreteconstruction.net/how-to/materials/concrete-reinforced-with-polypropylene-fibers_o

16. Barborak R., "Construction and Materials Tips," *Texas Department of Transportation* Accessed 19 July 2018 ftp://ftp.dot.state.tx.us/pub/txdot-info/cst/tips/frc_4550.pdf

17. Hadi N.S., "An Investigation of the Behavior of Steel and Polypropylene Fibre Reinforced Concrete Slabs*," University of Wollongong* Accessed 19 July 2018 http://ro.uow.edu.au/cgi/viewcontent.cgi?article=1492&context=engpapers

18. "Eucon AEA-92 Air Entraining Agent for Concrete," *Euchlid Chemical* Accessed 20 July 2018 https://www.euclidchemical.com/fileshare/ProductFiles/TDS/Eucon_AEA_92.pdf

19. "Concrete Technology in Focus: Shrinkage of Concrete," *Master Builders Solutions* Accessed 19 July 2019 https://assets.master-builders-solutions.basf.com/Shared%20Documents/EB%20Construction%20Chemcials%20-%20US/Admixture%20Systems/Brochures/Shrinkage_Of_Concrete_CTIF.pdf

20. Idiart A.E., "Drying Shrinkage and Creep in Concrete: Summary," Accessed 20 July 2018 https://www.tdx.cat/bitstream/handle/10803/6263/TAEIC2de5.pdf

21. Ghosh S.R., "A hypothesis on mechanism of maturing creep of concrete," *Materialux et Construction,* Vol. 6, No. 1, pp23-27, 1973 https://link.springer.com/article/10.1007%2FBF02474839

22. Bazant P.Z., Prasannan S., "Solidification Theory for Aging Creep," *Cement and Concrete Research*, Vol. 18, pp. 923-932, 1988

23. Granger P. L., Bazant Z. P., "Effect of Composition on Basic Creep of Concrete and Cement Paste," *Journal of Engineering Mechanics* pp.1261-1270, 1995

24. Kumar A. G., Kumar N. S., "Creep of Concrete," *International Journal of Engineering Development and Research*, Vol. 2, No. 4, 2014

25. Qian C., Zhang Y., Huang H., Qu J., Guo J., "Influences of Superplasticizers on Basic and Drying Creep of Concrete," *Structural Concrete,* 2016
26. Bazant P.Z., Panula L, "Part IV: Temperature effect on basic creep," *Materials and Structures* Vol. 11, pp.425 – 434, 1978
27. ACI Committee 209, "Guide for Modeling and Calculating Shrinkage and Creep in Hardened Concrete," *American Concrete Institute (ACI209.R-08),* 2008
28. Bazant Z. P., Baweja S., "Creep and Shrinkage Prediction Model for Analysis and Design of Concrete Structures: Model B3," *Adam Neville Symposium: Creep and Shrinkage- Structural Design Effect,* pp.1-83, 2001
29. Magnusson S. K., *Modeling of Creep in Hot-Cured Concrete Used in Prestressed, Precast Bridge Girders* M.S. Thesis, University of Washington, 2018, Web. Accessed 21 July 2019
30. Forth J.P., Ambrose E.E., "Influence of Relative Humidity on Tensile and Compressive Creep of Concrete Amended with Ground Granulated Blast-Furnace Slag," *Nigerian Journal of Technology* Vol 37, No. 1, pp.19-27, 2018
31. Kennedy, T., *Long Term Creep Behavior of Concrete and the Effects of Curing* Austin: Department of Civil Engineering, 1972. Print. 3661-2
32. Niyogi K. A., Hsu P., Meyers L. B., "The Influence of Age at the Time of Loading on Basic and Drying Creep," *Cement and Concrete Research* Vol. 3, pp.633-644, 1973
33. He Z., Qian C., Li L., Du S., "Creep Analysis of Concrete with Different Mineral Admixtures," *Materials Express* Vol. 6, No. 4, 2016

34. "Standard Test Method for Flexural Strength of Concrete (Using Simple Beam with Third Point Loading)," ASTM International C78 – 02 2002

35. Bassuoni T. M., Nehdi L. M., Greenough R. T., "Enhancing the Reliability of Evaluating Chloride Ingress in Concrete Using the ASTM 1202 Rapid Chloride Penetrability Test," *Journal of ASTM International* Vol. 3, No. 3, 2006

36. Castel A. Foster J. S., Ng T. Sanjayan G. J., Gilbert I. R., "Creep and drying shrinkage of a blended slag and low calcium fly ash geopolymer Concrete," *Materials and Structues* Vol. 49, No. 5, pp.1619-1628, 2016

37. Orbe A., Cuadrado J., Losada R., Roji E., "Framework for the design and analysis of steel and fiber reinforced self-compacting concrete structures," *Construction and Building Materials* Vol. 35, pp. 676 – 686, 2012

38. Barragan B., Zerbino R., Gettu R., Soriano M., De La Cruz C., Giaccio G., Bravo Michael B., "Development and Application of Steel Fiber-Reinforced Self-Compacting Concrete," *6th Int. RILEM International Symposium on Fiber Reinforced Concrete,* Varenna, Italy, 2004

39. Aslani F., Nejadi S., "Creep and Shrinkage of Self-Compacting Concrete with and without Fibers," *Journal of Advanced Concrete Technology,* Vol. 11, pp.251-265, 2013